

T.R.N.C  
NEAR EAST UNIVERSITY  
INSTITUTE OF HEALTH SCIENCES

SPECTROPHOTOMETRIC AND POTENTIOMETRIC  
DETERMINATION OF ACID DISSOCIATION CONSTANT  
( $pK_a$ ) VALUES OF SOME NONSTEROIDAL  
ANTI-INFLAMMATORY DERIVATIVES OF  
3-SUBSTITUTED PIPERAZINOMETHYL  
BENZOXAZOLINONES

Semra ALTUNTERİM ERKAN

ANALYTICAL CHEMISTRY

MASTER'S PROGRAM THESIS

NICOSIA

2017



T.R.N.C

NEAR EAST UNIVERSITY

INSTITUTE OF HEALTH SCIENCES

SPECTROPHOTOMETRIC AND POTENTIOMETRIC  
DETERMINATION OF ACID DISSOCIATION CONSTANT  
( $pK_a$ ) VALUES OF SOME NONSTEROIDAL  
ANTI-INFLAMMATORY DERIVATIVES OF  
3-SUBSTITUTED PIPERAZINOMETHYL  
BENZOXAZOLINONES

Semra ALTUNTERİM ERKAN

ANALYTICAL CHEMISTRY

MASTER'S PROGRAM THESIS

Advisor:

Assoc.Prof.Dr.Hayati ÇELİK

NICOSIA

2017

## ACKNOWLEDGMENTS

First and foremost I sincerely thank my master supervisor, Assoc. Prof. Hayati Çelik, who had supported me with sharing his great experience, and had helped me every process for my work.

I appreciate to Assist.Prof.Hürmüs Refiker and Assist.Prof.Usama Alshana for being my jury member, and would like to express my appreciation to Prof.Hakkı Erdoğan and Prof.Erhan Palaska for providing the studied chemicals. Also, I thank to all the members of the faculty of pharmacy at Near East University.

Also special thanks to Aysu Merve Nalbur, Başak Gizer, Alpcan Eroglu, Nilay Aleyna Durmaz, Halise Ebrar Hekimoğlu, and Birnur Güzeldağ from Yeditepe University and Dr. Abdikarim Abdi, Louai M. Saloumi, Emine Erdağ from Near East University for helping me during my thesis.

I would also like to thank my parents for their helps, love and endless patience in my motivation.

Finally, I would like to thank my husband, Özgür Erkan, who was always there cheering me up and stood by me through the good and bad times.

## ABSTRACT

### **Spectrophotometric and Potentiometric Determination of Acid Dissociation Constant ( $pK_a$ ) Values of Some Nonsteroidal Anti-inflammatory Derivatives of 3-substituted Piperazinomethyl Benzoxazolinones**

Acid dissociation constant ( $pK_a$ ) values of twenty structurally related 3-(4-substituted piperazinomethyl) benzoxazolinone derivatives (*HH01-20*) have been found by using UV-VIS spectrophotometry, and the results have been verified by potentiometric titration. The position of the equilibrium reaction was suggested based on the experimental evidence. Analgesic activities of molecules were compared with  $pK_a$  values of molecules. Due to the acidic and / or basic character of the compounds that show different activities, the ionization degrees of them could be determined by pH values and acidity constant with regarding its medium.

Our results suggest that analgesic/anti-inflammatory activities of *HH01-20* changed when the  $pK_a$  values of compounds were changed. Based on the data, the electro withdrawing groups (chlorine or fluorine atom) on benzoyl derivatives at the 6<sup>th</sup> position of benzoxazolinone or on the main structure of benzoxazolinone ring showed more basic character. Acetyl substituted derivatives have shown more basic characters than the others structures and have given more pharmacologic activities.

**Key words:** Acidity constant,  $pK_a$ , UV-VIS spectrophotometer, potentiometric titration, 3-(4-substituted piperazinomethyl) benzoxazolinone, activity-structure relationship

## ÖZET

### **Bazı 3-Piperazinometil Benzoksazolinon Türevlerinin asit iyonlaşma sabitlerinin ( $pK_a$ ) Spectrofotometrik ve Potansiyometrik Yöntemler ile Belirlenmesi**

Yirmi yapısal olarak ilişkili 3-(4-piperazinometil) benzoksazolinon türevlerinin asit iyonlaşma sabitlerinin ( $pK_a$ ) UV-VIS spektroskopisi kullanılarak bulunmuş ve sonuçlar potansiyometrik titrasyon yöntemi kullanılarak doğrulanmıştır. Denge reaksiyonunun konumu, deney sonuçları temel alınarak önerilmiştir. Moleküllerin analjezik etkinlikleri, moleküllerin  $pK_a$  değerleri ile karşılaştırılmıştır. Farklı aktivite gösteren bileşiklerin asidik ve/veya bazik karakterleri nedeniyle, iyonlaşma miktarı ortamın pH değerleri e asitlik sabitine göre belirlenebilir.

Sonuçlarımız, bileşiklerin  $pK_a$  değerleri değiştiğinde benzoksazolinonun analjezik / anti-inflamatuar aktivitelerinin değiştiğini göstermektedir. Verilere dayanarak, benzoksazolinon halkasının 6. pozisyonuna bağlı benzoil türevleri üzerindeki ya da benzoksazolinon halkası üzerinde electron çeken gruplar (klor veya flor atomu gibi) daha bazik bir karakter gösterdi. Asetil sübstitüsyonlu türevler diğer yapılardan daha bazik özellik göstermiş ve daha fazla farmakolojik aktiviteye sahip olduğu gözlenmiştir.

**Anahtar kelimeler:** Asitlik sabiti,  $pK_a$ , UV-VIS spektrofotometri, potansiyometrik titrasyon, 3-(4-piperazinometil) benzoksazolinon.

<b>TABLE OF CONTENTS</b>	<b>Page No:</b>
<b>APPROVAL</b> .....	iii
<b>ACKNOWLEDGMENTS</b> .....	iv
<b>ABSTRACT</b> .....	v
<b>ÖZET</b> .....	vi
<b>TABLE OF CONTENTS</b> .....	vii
<b>TABLE OF FIGURES</b> .....	viii
<b>LIST OF TABLES</b> .....	viii
<b>LIST OF SCHEMES</b> .....	ix
<b>SYMBOLS AND ABBREVIATIONS</b> .....	xi
<b>1.OVERVIEW</b> .....	1
<b>2.INTRODUCTION</b> .....	4
<b>2.1.General Structure of Benzoxazolinone</b> .....	4
<b>2.2.Synthesis Methods and Chemical Properties</b> .....	4
<b>2.3Acid-Base Chemistry</b> .....	6
<b>2.4.Ionization Constant Assignment Methods</b> .....	12
<b>2.5. UV–VIS spectrophotometry</b> .....	12
<b>2.6. Potentiometric Method</b> .....	22
<b>3. EXPERIMENTAL PART</b> .....	24
<b>3.3.Chemicals Used in Analysis</b> .....	27
<b>3.4. Equipments</b> .....	27
<b>3.5. Buffer solutions</b> .....	27
<b>3.6. Experimental methods</b> .....	28
<b>3.6.1.Ultraviolet–Visible region (UV-VIS) spectroscopy method</b> .....	29
<b>3.6.2Potentiometric method</b> .....	28
<b>4. RESULTS</b> .....	30
<b>5. DISCUSSION</b> .....	45
<b>6. CONCLUSION and RECOMMENDATION</b> .....	48
<b>REFERENCES</b> .....	51

**TABLE OF FIGURES**

**Page No:**

<b>Figure 1.1.</b> Pathway Of Prostanoid Synthesis From Arachidonic Acid .....	2
<b>Figure 2.1.</b> General Structure Of 2-(3H)-Benzoxazolinone .....	4
<b>Figure 4.1.</b> Absorbance vs. Wavelength Plot For $3 \times 10^{-5}$ M <i>HH01</i> In Various Buffers .....	32
<b>Figure 4.2.</b> Plot Of Absorbance As A Function Of pH for <i>HH01</i> at 288 nm .....	33
<b>Figure 4.3.</b> Potentiometric Titration Curve For <i>HH02</i> .....	34
<b>Figure 4.4.</b> Absorbance Vs. Wavelength Plot For $3 \times 10^{-5}$ M <i>HH02</i> In Various Buffers .....	36
<b>Figure 4.5.</b> Plot Of Absorbance As A Function Of Ph For <i>HH02</i> at 330 nm.....	37
<b>Figure 4.6.</b> Absorbance Vs. Wavelength Plot For $3 \times 10^{-5}$ M <i>HH07</i> In Various Buffers .....	38
<b>Figure 4.7.</b> Plot Of Absorbance As A Function of pH For <i>HH07</i> At 340 nm.....	39
<b>Figure 4.8.</b> Absorbance Vs. Wavelength Plot For $3 \times 10^{-5}$ M <i>HH13</i> In Various Buffers .....	40
<b>Figure 4.9.</b> Potentiometric Titration Curve For <i>HH13</i> .....	41
<b>Figure 4.10.</b> Absorbance Vs. Wavelength Plot For $0.75 \times 10^{-5}$ M <i>HH18</i> In Various Buffers.....	42
<b>Figure 4.11.</b> Absorbance vs. Wavelength Plot For $1 \times 10^{-5}$ M <i>HH20</i> In Various Buffers.....	43
<b>Figure 4.12.</b> Plot Of Absorbance Values As A Function Of Ph For <i>HH20</i> at 250 nm.....	44



<b>LIST OF TABLES</b>	<b>Page No:</b>
<b>Table 2.1.</b> Electronic Transition Involving $n, \sigma$ and $\pi$ Molecular Orbital .....	15
<b>Table 3.1.</b> Structural Formulas Of The 3-(4-Substituted Piperazinomethyl) Benzoxazolinone Derivatives .....	24
<b>Table 4.1.</b> The Experimental $pK_a$ Values Of 3-(4-Substituted Piperazinomethyl) Benzoxazolinone Derivative .....	31
<b>Table 5.1.</b> The $pK_a$ and Analgesic Activity Values For <i>HH01-HH05</i> and ASA .....	46
<b>Table 5.2.</b> The $pK_a$ and Analgesic Activity Values For <i>HH06-HH08</i> and ASA .....	46
<b>Table 5.3.</b> The $pK_a$ and Analgesic Activity Values For <i>HH10-HH13</i> and ASA .....	47
<b>Table 5.4.</b> The $pK_a$ and Analgesic Activity Values For <i>HH14-HH19</i> and ASA .....	47
<b>Table 6.1.</b> The $pK_a$ and Analgesic Activity Values For <i>HH01, HH11, HH14</i> and ASA .....	48

**LIST OF SCHEMES****Page No:**

<b>Scheme 4.1.</b> Equilibrium For The Protonation of 3-(Substitute Piperazinomethyl benzoxazolinone( <i>HH01</i> ) .....	35
---	----

**SYMBOLS AND ABBREVIATIONS**

<b>A</b>	<b>Absorbance</b>
<b>K<sub>a</sub></b>	<b>Acid dissociation constant</b>
<b>K<sub>b</sub></b>	<b>Base dissociation constant</b>
<b>ASA</b>	<b>Acetylsalicylic acid</b>
<b>C</b>	<b>Concentration</b>
<b>COX</b>	<b>Cyclooxygenase enzyme</b>
<b>I</b>	<b>Ionic strength</b>
<b>λ</b>	<b>Wavelength</b>
<b>NSAIDs</b>	<b>Nonsteroidal anti-inflammatory drugs</b>
<b>b</b>	<b>Path length</b>
<b>π</b>	<b>Pi bond</b>
<b>P</b>	<b>Power</b>
<b>PG</b>	<b>Prostaglandine</b>
<b>σ</b>	<b>Sigma bond</b>
<b>T</b>	<b>Transmittance</b>
<b>UV</b>	<b>Ultraviolet</b>
<b>VIS</b>	<b>Visible</b>

## 1. OVERVIEW

Nonsteroidal anti-inflammatory drugs (NSAIDs) are among the most widely used medications in the world due to their demonstrated efficacy in reducing pain and inflammation (Laine, 2001, p. 594). NSAIDs have a crucial role in management and treatment of many diseases and disorders as headaches, dental pain management, osteoarthritis, rheumatoid arthritis, dysmenorrhea, ankylosing spondylitis, gout, (Zochling et al., 2006, p. 423; Kean and Buchanan, 2005, p. 343).

NSAIDs act by inhibiting pro-inflammatory enzyme cyclooxygenase (COX). NSAIDs can be classed into traditional nonselective NSAIDs (tNSAIDs) inhibiting both COX isoenzymes, and selective COX-2 isoenzyme inhibitors. Although their effectiveness in many clinical conditions, tNSAIDs are associated with a significant risk of serious gastrointestinal adverse events as used on chronic bases (Ofman et al., 2002, p. 804). Yet, NSAIDs are considered to be a cornerstone therapy for the management of pain for both inpatients and outpatients or home use worldwide. NSAIDs work effectively in many pain associated conditions and thus prescribed for diverse medical conditions such as musculoskeletal pain, as well as for cancer associated pain, AIDS, surgery and post prosthetic devices placement rehabilitation (Bryant et al., 2017). Though the deleterious and frequent gastrointestinal side effects of tNSAIDs are to be a major limitation for their use, specific inhibitors of the COX-2 isoenzyme were developed, thus opening the possibility to provide anti-inflammatory and analgesic benefits, while theoretically not affecting the gastro-protective role of COX-1 isoenzyme activity. Several side effects are associated with NSAID administration and use, of mention are hepatic injury and platelet inhibition which may result in increased bleeding, also their effect on blood pressure and alterations in renal function. Yet the most relevant adverse effects of tNSAIDs and COX-2 inhibitors are respectively the gastrointestinal and cardiovascular side effects (Lo and Meadows, 2006, p. 260; Mamdani et al., 2003, p. 481). Metabolism of arachidonic acid to prostaglandins and related lipid mediators is carried by two separate COX gene products, COX-1 and COX-2 (Zuniga et al., 2004, p. 806). In most body tissue COX-1 is expressed where it mainly regulates the homeostatic

production of arachidonic acid metabolites needed to maintain physiologic integrity, involving gastric cytoprotection carried by prostacyclin ( $\text{PGI}_2$ ) (Figure 1.1). COX-2 is formed in response to inflammatory stimuli, leading to increased production of eicosanoid mediators for inflammation and pain. All tNSAIDs restrain COX-2 and in addition COX-1 for shifting degrees and are associated with high risk of gastrointestinal ulcers and more fatal upper gastrointestinal complications (Dubois et al., 1998, p. 1063; Langman et al., 1994, p. 1075).



**Figure 1.1. Pathway of prostanoid synthesis from arachidonic acid**

The ulcerogenic properties of tNSAIDs mainly are due to their ability to inhibit the function of COX-1 in the gastric mucosa (Wolfe et al., 1999, p. 1888), as agents tend to be COX-1 sparing, i.e. COX-2 selective, express less gastrointestinal toxicity. Studies reported 15% to 30% of patients who regularly use tNSAIDs to develop gastric or duodenal ulcer as confirmed using endoscopy (Laine, 2001, p. 594).

Many reports indicate that compounds containing the benzoxazolinone ring possess analgesic and anti-inflammatory activities (Brunet and Cazin, 1981, p. 604). It has been shown that some synthesized 3-(4-substituted piperazinomethyl) benzoxazolinone derivatives that have analgesic, anti-inflammatory activity and inhibit prostaglandin  $\text{E}_2$  ( $\text{pGE}_2$ ) induced edema (Pilli et al., 1993, p. 1351). The research has been continued to find new nonsteroidal anti-inflammatory compounds

having analgesic and anti-inflammatory activity with less gastrointestinal effects and toxicities.

Active pharmaceutical ingredients (APIs) are among the so-called “emerging” harmful substances that are being studied in recent years. They are causing the harm to environment while production, or disposal of unused or expired drugs. Their bioactive metabolites cause harm to animals and sub marine life by present participle of sediment in the soil and water.

Because most APIs pose acidic and basic functionalities, their ionization state is determined by both solution pH and dissociation constants. Anionic usually have different properties such as volatility, water solubility, UV absorption, and reactivity with chemical oxidants. The ionized form is more water soluble, while the neutral form is more lipophilic and has higher membrane permeability. The ionization of the substance plays vital role in the distribution, absorption, metabolism and compounds in biological systems and the environment. From dissociation constants, the major species of pharmaceuticals present in the environment (usually in neutral pH range) can be estimated (Pool et al., 2004, p. 445). Consequently, it is very important to know dissociation constants for environmentally relevant active pharmaceutical ingredients in order to estimate their occurrence, fate and effects.

Furthermore, the acid–base property of a drug molecule is the key parameter for drug development because it governs solubility, absorption, distribution, metabolism and elimination.  $pK_a$  is the fundamental parameter for the transport of the drugs into and across membranes (Andrasi et al., 2007, p. 1040).

In this thesis project we aim first to determine the  $pK_a$  values of twenty 3-(4-substituted piperazinomethyl) benzoxazolinone derivatives using spectrophotometric methods. Potentiometry is used later to confirm acidity constants obtained. The relevance of this project lays in the importance of determining the acidity constant of the studied compounds thus to further understand their chemical characteristics and other pharmacological effects. Furthermore, we also discuss the relationship between the acidity constant and analgesic/anti-inflammatory activities of these drug candidates.

## 2. INTRODUCTION

### 2.1. General Structure of Benzoxazolinone

2-(3H)-Benzoxazolinone compound is composed of benzene and 2-oxazolone rings. Classical numbering of the molecule is shown in Figure 2.1.

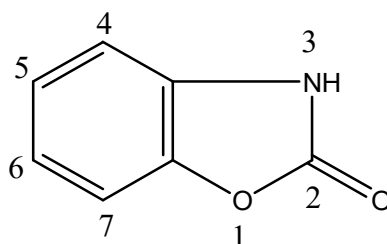


**Figure 2.1. General structure of 2-(3H)-Benzoxazolinone**

### 2.2. Synthesis Methods and Chemical Properties

In the synthesis, benzoxazolinone or 5-chloro benzoxazolinone reacts with an appropriate carboxylic acid in polyphosphoric acid (PPA). Polyphosphoric acid is highly viscous acid, which is mainly used for acylations and heterocyclic synthesis in organic chemistry. As a result, in the first step benzoxazolinone ring is acylated at 6<sup>th</sup> position (Figure 2.2).

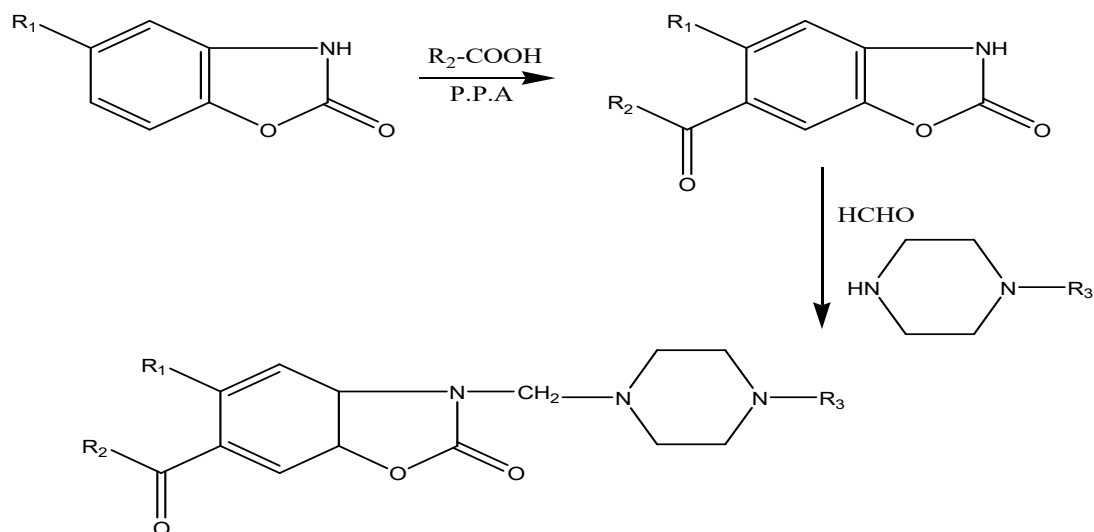


**Figure 2.2. General synthesis mechanism of 3-(4-substituted piperazinomethyl benzoxazolinone derivatives.**

The second step is an example of Mannich reaction where the active hydrogen of secondary amino group at 3rd position of 6-acyl benzoxazolinone and the other active hydrogen on piperazine derivative react with the carbonyl oxygen of formaldehyde giving one molecule of water.

This is a condensation reaction that two different compounds having active hydrogens (6-acyl benzoxazolinone and the piperazine derivative) combined via methylene bridge (–CH<sub>2</sub>–). As a result, synthesis of 6-cylated 3-(4-substituted piperazinomethyl) derivatives of benzoxazolinones have been published in the literature (Palaska et al., 1995, p. 693).

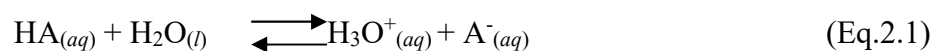


### 2.3. Acid-Base Chemistry

Acid-base reactions are ubiquitous. Power of acids and bases can be distinguished in this way, and their differences can be assessed. This also allows comparisons and qualitative assessments (Alber, 1984).

Organic compounds can contain acidic or basic groups, which determine the chemical, physical, and biological properties of the compound. In such compounds, the ratio of molecular, anionic and cationic types to each other can be calculated by using equilibrium constant,  $K$ , values. Moreover, distinguishing substances that are chemically alike can be realized with the help of  $K$  values.

By measuring the equilibrium constant of acids ( $K_a$ ) in aqueous solutions; the relative strengths of acids could be quantified. When solutions contain the same concentrations, the stronger acids ionize to a greater extent than weak acids, and thus yield higher concentrations of hydronium ions ( $H_3O^+$ ) than the weaker. Acid dissociation constant,  $K_a$ , is defined as the equilibrium constant for an acid. If we assume the reaction of an acid (HA) as follows:



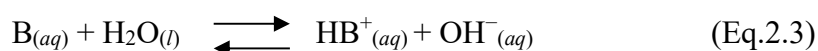
Then the equation for the ionization constant will be as follows:

$$K_a = \frac{[H_3O^+][A^-]}{[HA]} \quad (\text{Eq.2.2})$$

The concentrations are all at equilibrium. Here, the concentration of water is not added or included in the equation though it is a reactant in the reaction. A larger

ionization constant will be for a stronger acid than does a weaker acid, as the strengths of the acids increase, ionization constants will increase.

We can rank the strengths of bases by their tendency to form hydroxide ions in aqueous solution. The reaction of a Brønsted-Lowry base with water is given by:



Water acting as an acid will react with the base B forming  $HB^+$ , which is the conjugated acid of the base B, while the hydroxide ion  $OH^-$  forms the conjugated base of water. Strong bases, such as sodium hydroxide (NaOH), are considered strong electrolyte) due to their complete dissociation when dissolved in water; thus, yielding 100% of  $OH^-$  and  $HB^+$  when NaOH reacts with water. However, a weak base yields a small proportion of hydroxide ions in the solution. When the weak base dissolves in the water, base ionization constant ( $K_b$ ) is the key parameter in measuring the relative strength of base in aqueous solutions. In the same manner stronger bases ionize to a larger extent yielding greater hydroxide ion concentrations compared to weaker bases in solutions of the same concentration (Flowers et al, 2015, p. 777). Here the equation for the ionization constant ( $K_b$ ) will be as follows:

$$K_b = \frac{[HB^+][OH^-]}{[B]} \quad (\text{Eq.2.4})$$

Conjugate base and weak acid form a buffer solution. A buffer solution is a solution formed from a mixture of a weak acid and its conjugate base (or vice versa) cause hindrance in change of pH after addition of small amounts of a strong base or a strong acid. Two examples are a solution of ammonia ( $NH_3$ ) and ammonium chloride ( $NH_4Cl$ ) or a solution of acetic acid ( $CH_3COOH$ ) and sodium acetate ( $CH_3COONa$ ), the first is a buffer that consists of a weak base and its salt while the last is an

example of a buffer which consists of a weak acid and its salt (Flowers et al, 2015, p. 777).

The ionization constant ( $K_a$ ) of acetic acid is greater than the  $K_b$  of its conjugate base so this weak acid solution with its salt is acidic. Being a buffer it contains both the weak acid and its salt which keep the hydronium ion concentration (and the pH) almost constant by adding either a little amount of a strong base or a strong acid (Flowers et al, 2015, p. 777). If for instance strong base like NaOH is added, the hydroxide ion reacts with the few hydronium ions present that lead acetic acid to react with water, thus restoring the hydronium ion concentration to its original value:



Minor change will occur on the pH. When we add a strong acid such as concentrated hydrochloric acid (HCl), most of the hydronium ions will bind with acetate ions, forming acetic acid molecules:



Consequently, there is very little increase in the concentration of the hydronium ion, and the pH remains practically unchanged as show in Figure 2.3.

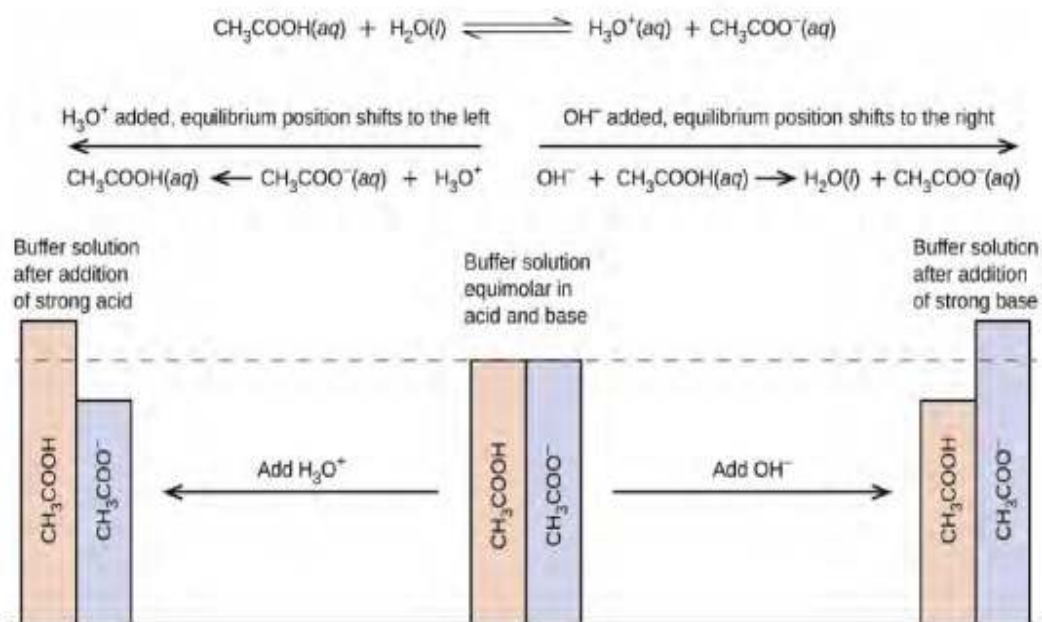
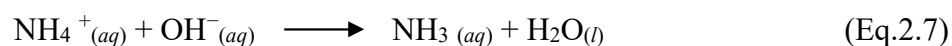
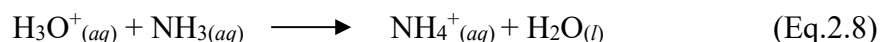


**Figure 2.3. The diagram of the buffer action.**

A second example for buffers is the mixture of ammonia and ammonium chloride which contains the salt of the weak base. The solution is basic as the ionic concentration  $K_b$  for ammonia is larger than the ionic concentration  $K_a$  for the ammonium ion. If we add a strong base as  $\text{OH}^-$  ions, ammonium ions in the buffer solution react with the  $\text{OH}^-$  ions to form ammonia and water, thus minimize the  $\text{OH}^-$  ion concentration nearly to its previous value before addition:



Whereas in the addition of an acid (hydronium ions), ammonia molecules get into reaction with the hydronium ions thus producing ammonium ions while decreasing the concentration of hydronium ion nearly to its value before addition of acid:



However, buffer solutions have a limit capacity for tolerating acid or base addition while keeping pH relatively constant. In the case of adding a strong base or a strong acid to a buffer solution to the extent that the weak acid or weak base is exhausted, the function of buffer solution is unable. In fact, we do not even need to exhaust all of the acid or base in a buffer to overwhelm it; its buffering effect will decline quickly as a given component diminished.

The quantity of acid or base that could be added to a specific volume of a buffer solution before the value of pH changes significantly (mainly by 1 pH unit) is called the *buffer capacity*. It depends mainly on the quantities of the weak acid and its conjugate base that are present in buffer solutions. For instant, if we assume one liter of a solution having 1.0 M of acetic acid and 1.0 M of sodium acetate it will then have a greater buffer capacity than one liter of a solution that is 0.10 M of acetic acid and 0.10 M of sodium acetate even though both solutions have the same pH value. Containing more acetic acid and acetate ion is what makes the first solution to have more buffer capacity.

***The Henderson-Hasselbalch Equation:*** The ionization-constant expression for a solution of a weak acid could be give as in Eq.2.2. Rearrangement to solve for  $[\text{H}_3\text{O}^+]$ , one can get:

$$[\text{H}_3\text{O}^+] = K_a \times \frac{[\text{HA}]}{[\text{A}^-]} \quad (\text{Eq.2.9})$$

Taking the negative logarithm of both sides of this equation, we arrive at:

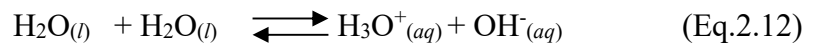
$$-\log [\text{H}_3\text{O}^+] = -\log K_a - \log \frac{[\text{HA}]}{[\text{A}^-]} \quad (\text{Eq.2.10})$$

which can be rewritten as:

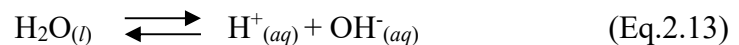
$$pH = pK_a + \log \frac{[A^-]}{[HA]} \quad (\text{Eq.2.11})$$

where  $pK_a$  is the negative of the common logarithm of the ionization constant of the weak acid ( $pK_a = -\log K_a$ ). This equation called the ***Henderson-Hasselbalch equation*** relates the pH, to the weak acid and its salt concentrations with the value of the ionization constant of a weak acid in a buffered solution. Researchers frequently use this expression for calculating the pH of buffered solutions (Flowers et al, 2015, p. 777).

In pure water, not containing any added electrolytes, a small electrical conductivity appears showing the presence of ions, said to be the autoionization effect of water.



The hydrated hydrogen ion is considered as hydronium. There is never “just a proton” in solution. However, the hydronium ion is often represented by “just a proton” and the autoionization is written as a dissociation reaction.



For the above reaction, one can write the equation for the water dissociation constant as follows:

$$K_w = [H^+] [OH^-] = 1 \times 10^{-14} \text{ at } 25 \text{ }^\circ\text{C} \quad (\text{Eq.2.14})$$

If we multiply  $K_a$  of HA with  $K_b$  of its conjugate base  $A^-$ , that gives  $K_w$ . For conjugate-acid base pairs, the acid dissociation constant  $K_a$  and base ionization constant  $K_b$  can be correlated by the following equations:

$$pK_a + pK_b = pK_w \quad (\text{Eq.2.15})$$

$$pK_a + pK_b = 14.00 \quad (\text{Eq.2.16})$$

#### 2.4. Ionization Constant Assignment Methods

Several methods exist for the determination of dissociation constants. Classically potentiometry (Qiang and Adams, 2004, p. 2874; Wróbel and Chmurzyński, 2000, p.303) and UV–VIS absorption spectrophotometry used to be the most preferable methods due to their accuracy and reproducibility for quantifying equilibrium constants (Beltran et al., 2003, p. 253).

#### 2.5. UV–VIS spectrophotometry

Lower solubility compounds and lower sample concentrations can be sort out by the Spectrophotometric methods which is UV–VIS spectrophotometry. The high sensitivity ( $>10^{-6}$  M) to compounds plus favorable molar absorption coefficients is considered its main advantage. It must be clear that, a compound should contain a UV-active chromophore that must be close enough to the site of the acid–base function in the compound.

These experiments can be carried by several ways. An instrument will be used during titration to continuously record spectral data. As the process of titration continues; the absorption spectra of the sample changes, reflecting the concentrations of ionized and neutral species present in the solution.

As the pH corresponding to a  $pK_a$  value is approached the largest change in absorbance takes place. These changes are mainly determined from overlay plots of the different spectra or from the first derivative of the absorbance against time plot.

The quantification of  $pK_a$  values by UV–VIS assumes that the concerned solute to be pure or to contain impurities not affecting since not being absorbed in the UV–VIS range, because the spectra of impurities can often overlap with those corresponding to the solutes of interest (Jime'nez-Lozano et al., 2002, p. 37; Völggi, et al., 2007, p. 418). Another way to use an UV-VIS spectrophotometric method is that the spectral data is obtained at a single analytical wavelength from a sample in a series of buffer solutions with known pH values, after which the  $pK_a$  can be determined. For carrying such an experiment, the absorption spectra must be procured before and the molar absorptivities of neutral species and protonated species are considered some time. These estimations are non-trivial if acid-base equilibria involve more than two ionization steps or responding parts are not steady inside two pH units of the  $pK_a$  esteem. Recently a multi-wavelength spectrophotometric technique for measuring a corrosive separation consistent was produced. Target-factor investigation has been connected to reason  $pK_a$  esteems from the multi-wavelength UV assimilation information recorded at various pH esteems (Allen et al., 1998, p. 699).

Earliest spectroscopic studies were carried by characterizing the emission of visible light, from flames, from salts added to flames and visible light from the sun. Spectroscopy starts with absorption in which a beam of electromagnetic radiation passes through a sample and transmitted mostly without a loss in intensity. Yet at selected frequencies as the radiation's intensity is attenuated, this attenuation is called the *absorption process*.

For an analyte to absorb electromagnetic radiation, two requirements should be established. First the radiation's electric field or magnetic field interaction with the analyte should be assured. For visible radiation and ultraviolet radiation, this interaction involves the electronic energy of valence electrons. The absorbance of infrared radiation alters chemical bond's vibrational energy. Secondly, the energy of



the difference of energy between two states is presented as  $\Delta E$ , which is the energy of electromagnetic waves.

The simple demonstration of the photons is illustrated in the Figure 2.4 (Harvey, 2000. p. 381). It is clear that the energy of low- energy and high energy levels must be equal to the energy of the photons. Till now the data for the types of energy levels involved and transition states and appearance of the resulting spectrum is is not clear.

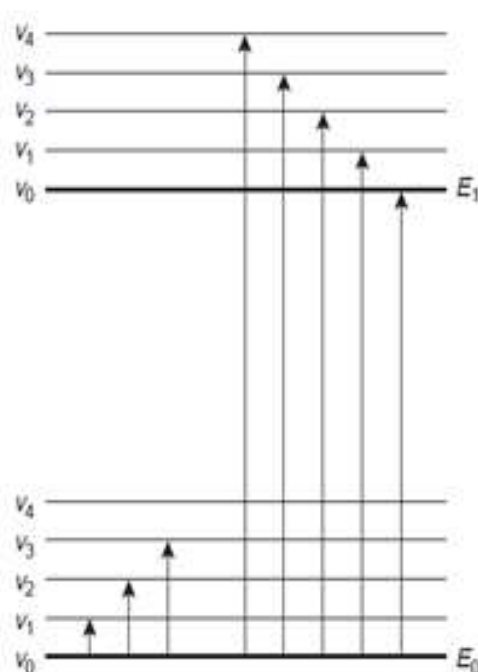


**Figure 2.4. Energy level diagram shows difference between the absorption of infrared radiation (left) and ultraviolet – visible radiation (right).**

The energy levels are considered as absorbance levels and each level represents the vibrational energy level. With  $E_0$  and  $E_1$  being the lowest energy level and the high respectively.

UV-VIS spectra for molecules and ions undergo a change in its valence electron configuration when absorbs ultraviolet or visible radiation. The valence

electrons occupy quantized sigma bonding,  $\sigma$ , pi bonding,  $\pi$ , and nonbonding,  $n$ , molecular orbitals in organic molecules, and inorganic anions. Unoccupied sigma antibonding,  $\sigma^*$ , and pi antibonding,  $\pi^*$ , whereas molecular orbitals often lie close enough in energy that the transition of an electron from an occupied to an unoccupied orbital is possible.

UV-VIS spectra have four types of transitions between quantized energy levels. The approximate wavelength ranges for these absorptions is shown in Table 2.1 (Harvey, 2000. p. 382).

**Table 2.1. Electronic transition Involving  $n$ ,  $\sigma$  and  $\pi$  molecular orbitals.**

Transition	Wavelength Range (nm)	Examples
$\sigma \longrightarrow \sigma^*$	< 200	C–C, C–H
$n \longrightarrow \sigma^*$	160 – 260	H <sub>2</sub> O, CH <sub>3</sub> OH, CH <sub>3</sub> Cl
$\pi \longrightarrow \pi^*$	200 – 500	C=C, C=O, C=N, C=C
$n \longrightarrow \pi^*$	250 – 600	C=O, C=N, N=N, N=O

The most important transitions are the  $n \rightarrow \pi^*$  and  $\pi \rightarrow \pi^*$ , the functional group and are available as analyte and sample characteristics. A chromophore is said to the bonds and functional groups which give rise to the absorption of visible radiation and ultraviolet radiation.

Transmittance (T) is defined as the ratio of the radiant power passing through a sample to that from the source of radiation as shown in Figure 2.5 (Harvey, 2000, p. 384).

Transmittance and absorbance (A) are the terms used to quantitatively describe the attenuation of electromagnetic radiation as it passes through a sample, transmittance is defined as the ratio of the electromagnetic radiation's power exiting the sample,  $P_T$ , to that incident on the sample from the source,  $P_0$ ,

$$T = \frac{P_r}{P_0} \quad (\text{Eq.2.17})$$

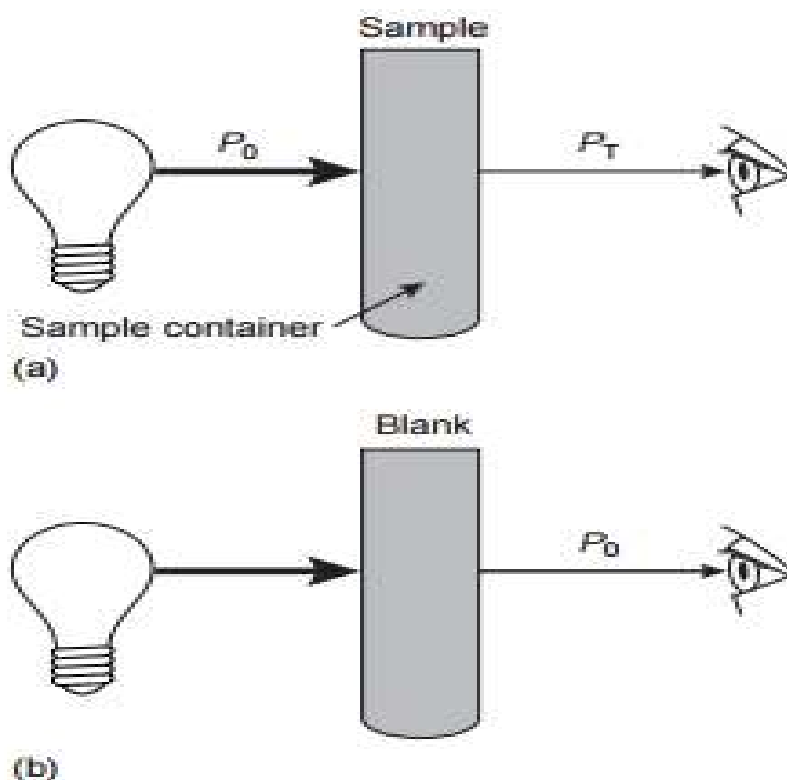


**Figure 2.5. (a) Schematic diagram showing the attenuation of radiation passing through a sample;  $P_0$  is the radiant power from the source and  $P_T$  is the radiant power transmitted by the sample. (b) Schematic diagram showing that  $P_0$  is redefined as the radiant**

Multiplying the transmittance by 100 gives the percent transmittance (%T), which varies between 100% (no absorption) and 0% (complete absorption). All detection devices either the human eye or a modern photoelectric transducers measure the transmittance of electromagnetic radiation. A transmittance of less than 1 occur when the energy is losses its intensity in analyte. As described, Equation 2.17 does not distinguish between the different ways in which the attenuation of radiation

occurs. A few more phenomena may add to the net attenuation of radiation other than absorption by an analyte those incorporate sample container reflection and absorption, ingestion because of test lattice other than the analyte and the diffusing of radiation. To tackle the situation the Blank method is used. The radiation's power leaving from the method blank is taken to be  $P_0$ . Absorbance ( $A_n$ ) is characterized as:

$$A = -\log T = -\log \frac{P_r}{P_0} = \log \frac{P_0}{P_r} \quad (\text{Eq.2.18})$$

Thus Absorbance  $A$  is the most common unit used for expressing the attenuation of radiation since it is being a linear function of the analytes concentration. Filter photometers form the simplest instrument recently used for molecular UV-VIS absorption as given in Figure 2.6 (Harvey, 2000. p. 389).

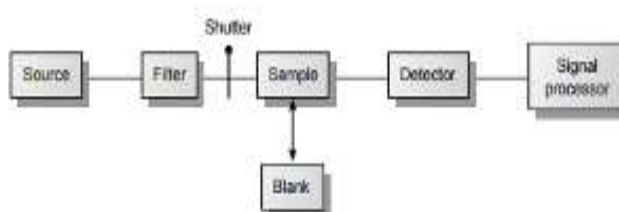


**Figure 2.6. Diagram for a filter photometer.**

To isolate a band of radiation a filter photometer uses an absorption or interference filter that is placed between the sources and sample thus avoiding its decomposition as exposed to high-energy radiation. Filter photometers are said to be single-beam instrument having a single optical path between the source and detector. It is calibrated to 0% T while using a shutter to block the source radiation from the detector, and then the instrument is calibrated to 100% T with a suitable blank after removing the shutter. Later we place the sample in place of the blank and measure its transmittance. Since the source's incident power and the sensitivity of the detector differ with varying wavelength, recalibration of the photometer is necessary

whenever we change the filter.

The advantage of photometers over other spectroscopic instruments relies mainly on; photometers relative reduces cost, portability, ruggedness and easy to maintain. However, the main disadvantage is their inability to generate an absorption spectrum

Spectrometers are instruments that use monochromators for wavelength selection. While a spectrophotometer is an instrument used in absorbance spectroscopy in which the transmittance is a ratio of two radiant powers. Single-beam instrument attached with a fixed wavelength monochromator are the simplest form of spectrophotometer as shown in Figure 2.7 (Harvey, 2000, p. 389).

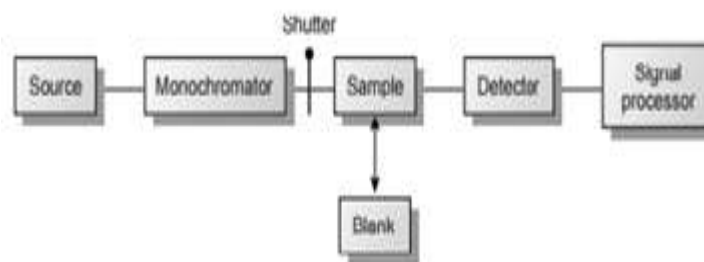


**Figure 2.7. Block diagram for a single-beam fixed wavelength spectrophotometer.**

The single beam photometer is used and a common example is Spectronic-20, with a set bandwidth of 20 nm and could use 340 to 625nm. Due to wide bandwidth it is preferable for the quantitative analysis than qualitative analysis spectrophotometers are available with an effective bandwidths of 2–8 nm.

Disadvantages of fixed-wavelength single-beam spectrophotometers are that it is not practical for recording spectra since it takes more time for manually adjusting the wavelength and recalibrating the spectrophotometer. Also their accuracy is limited by the stability of the beam source and detector over time. The use of the double-beam in-time spectrophotometer can minimize the limitations of fixed-wavelength, single-beam spectrophotometers given in figure 2.8 (Harvey, 2000, p.

390).

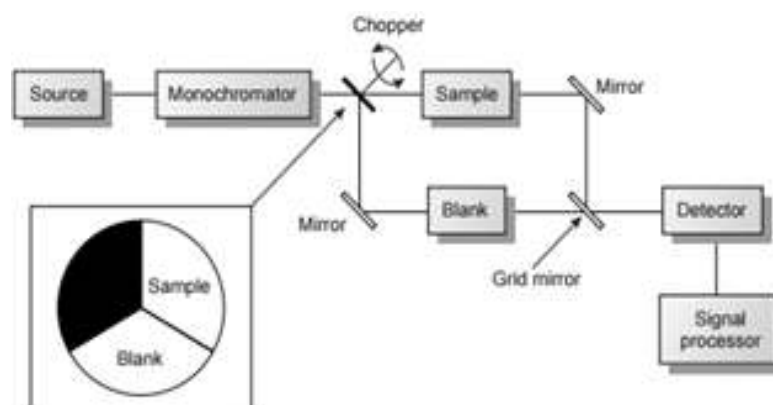


**Figure 2.8. Block diagram for a double-beam in-time scanning spectrophotometer.**

The radiation's way is controlled by a chopper, as the one appeared in the insert, which exchange it between the example, blank, and a shuttle. Utilizing the chopper's known speed of rotation the signal processor settle the signals achieving the detector into that from transmission of the blank ( $P_0$ ) and the specimen ( $P_T$ ). It is possible to continuously adjust the 0% T response of the detector by including an opaque surface as a shutter. Also using adjustable slits at the entrance and exit of the monochromator; it is conceivable to control effective bandwidth of a double-beam spectrophotometer. Usually successful bandwidth of between 0.2 nm and 3.0 nm are utilized. A scanning monochromator takes into consideration the recording of spectra. Double beam instruments are considered more versatile. The instrument designs considered up to this point utilize a single detector and can just check wavelength at any given moment (Harvey, 2000, p. 390).

An entire spectrum can be recorded in as little as 0.1 s using a linear photodiode array that consists of multiple detectors, or channels. Figure 2.9 illustrate a block diagram for a typical multichannel spectrophotometer. The radiation from the source is dispersed while passing through the solution by grating. The photodiode array record the wavelength of narrow range (Harvey, 2000, p. 390).

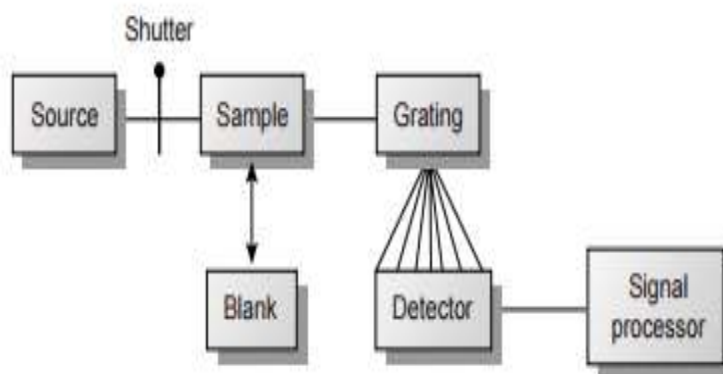


**Figure 2.9. Block diagram for a diode array spectrophotometer.**

The sample compartment for the instruments in Figures 2.6-2.9 provides a light-tight environment that prevents the loss of radiation, as well as the addition of stray radiation. Samples in liquid or solution state are placed in cells constructed with materials as quartz, glass, and plastic those are all UV-VIS transparent material.

When working at wavelengths of less than 300 nm; Quartz or fused-silica cells are required, since other materials show a significant absorption. Though cells with short path lengths ( $\geq 1$  mm) and long path lengths ( $\leq 10$  cm) exist yet the most common cell used has a path length of 1 cm. For the analysis of very dilute solutions and gasses the most useful cells are those with a longer path length. The highest quality cells are constructed in a rectangular shape, allowing the radiation to strike the cell at a  $90^\circ$  angle, where losses to reflections are minimal. For double-beam instruments cells which are available in matched pairs having identical optical properties, are the best fitting cells (Harvey, 2000, p. 391).

UV-VIS Spectroscopy can be used in qualitative and quantitative analysis. Quartz (silica) cells are generally used for analysis. In order for the best sensitive measurement in double beam path spectrophotometers, a pair of cells must be totally identical, some must be filled with pure solvent, the other with sample solution, and must be put into the places of the reference and sample. A solvent to be used for ultraviolet analysis must not make absorption in the same region with the compound

whose spectrum will be taken. If the difference spectrum deviates from the line present in times when the places for the sample and reference are empty, cells become non coherent. Therefore, cells must be calibrated for once, and the same cell must be used for the sample every time. Optic surfaces of the cells used must be well preserved. Touch of hand must be avoided, papers designed specifically for the cleaning of lens must be used, and paper towel must not be used. Cells must be filled and emptied with the help of a pipette; the content must not be poured from the cell. Once used, cells must be rinsed with water or ethanol, and must not be used if they have burrs and scratches on their surfaces. Procedures followed in UV-VIS spectroscopy measurements are given below:

1. Concentration is adjusted and an appropriate stock solution is prepared, then diluted in tampons having suitable pH values,
2. Pure spectrum which belongs to two ion types in balance is inquired,
3. Appropriate wavelength is elected for assignment (analytic wavelength),
4. Value close to  $pK_a$  value is studied,
5. Real value of  $pK_a$  is assigned

Assignment of ionization constant with UV-VIS Spectroscopy is based on the fact that types in balance make absorption in quite different wavelengths. Organic acids and bases give absorption spectrums according to the pH value of the environment. As HA is an organic acid, the balance and balance equality is given in Eq.2.1.

In terms of concentration, the equation formed when negative logarithms of both are taken is like the one given in Eq.2.11. In this equation, the value of  $pK_a$  can be measured if pH, [HA] and  $[A^-]$  are known.

This measurement can also be made without assigning the three unknowns separately. In the equation given in Eq.2.11, when  $[HA] = [A^-]$ ,  $pK_a = pH$ . Therefore, the value of the acidity constant ( $K_a$ ) can be found using the change of absorption with pH. Spectra formed by any compound according to pH can be obtained, and pH-absorption chart can be drawn with the help of these spectra (Figure 2.10).



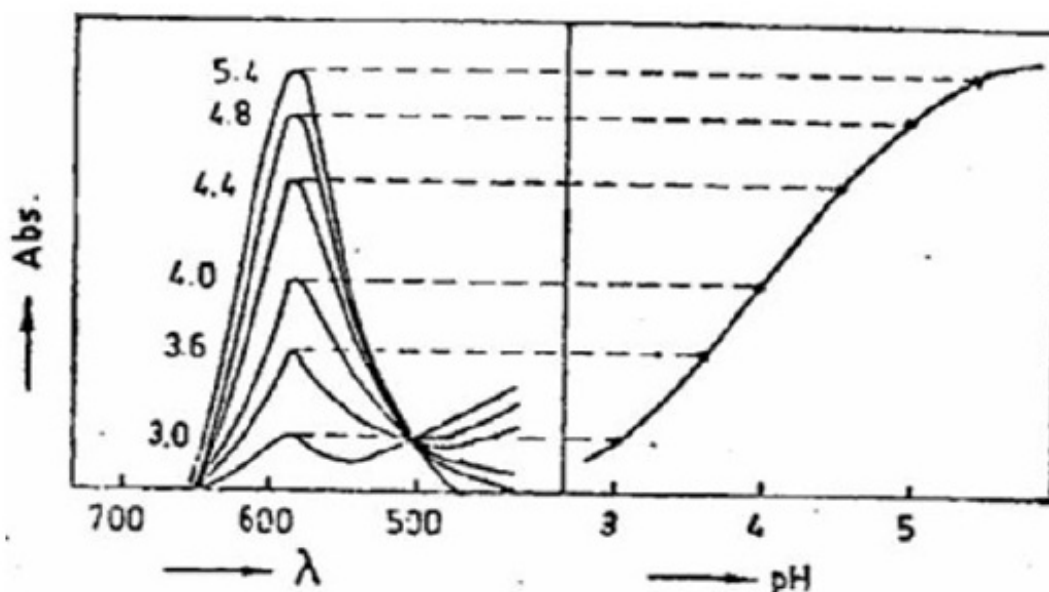


**Figure 2.10. Different pH values spectra of sample and creating pH – ABS. graphic from these spectra.**

pH-absorption chart given in Figure 2.10 is in sigmoid wave shape (S shape), and  $[HA] = [A^-]$  at the middle point of this chart. The lowest and highest absorptions of the chart must be determined to find the middle point. This point can be understood from the condition that, absorption with pH does not change any more. A parallel is drawn to the pH axis from the middle point, and then, a perpendicular is drawn from the point where this line cuts the sigmoid curve to the pH axis. The value showed by the perpendicular on pH axis is equal to  $pK_a$ .  $[HA] = [A^-]$  in the middle of the absorption and  $\log [A^-] / [HA] = 0$  (Skoog et al., 1998).

In another method used in  $pK_a$  assignment with spectrophotometric method,  $\log[(A - A_{\min}) / (A_{\max} - A)]$  values on a chosen wavelength are put into chart against the corresponding pH values. Thus,  $pK_a$  value is obtained directly with the place where the curve obtained by this chart cuts the abscissa axis (Helmy, 1997, p. 259).

## 2.6. Potentiometric Method

The potentiometric titration is the appropriate way of evaluation of  $pK_a$  values and pH electrode is used for titration. From the change in shape of the titration curve compared with that of blank titration without a sample; the  $pK_a$  value is calculated.

To derive  $pK_a$  from titration curves the following analysis methods are used commonly including Grans plot (Andrasi et al., 2007, p. 1040), second-derivative ( $D^2pH/DV^2$ ), and least squares non-linear regression (Qiang and Adams, 2004, p. 2874). The  $pK_a$  of a substance is calculated by the potentiometric titration. There is limitation of use in milligrams and use buffer solutions to detect considerable change the solution of  $10^{-4}$  M are needed. To avoid errors carbonate-free solutions must be for measurements at neutral-to-high pH values (Beltran et al., 2003, p. 253).

### 3. EXPERIMENTAL PART

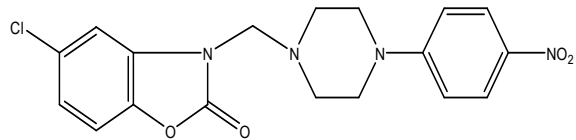
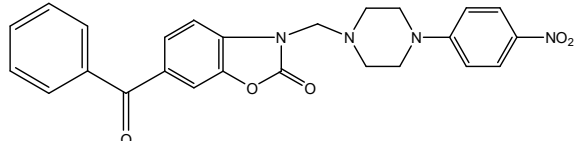
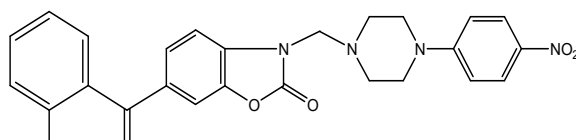
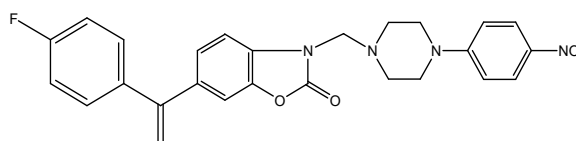
#### 3.1. Chemicals

All studied organic molecules used in this work are in analytic purity. No extra purification processes were applied to the chemicals used in this study.

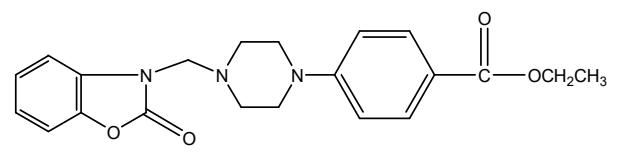
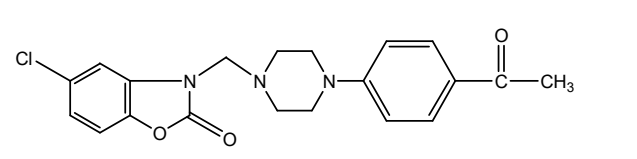
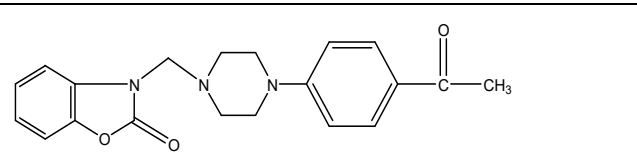
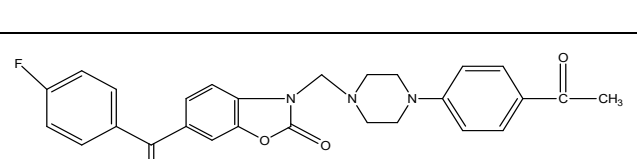
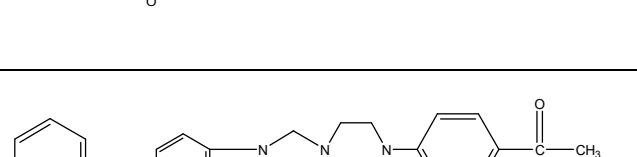
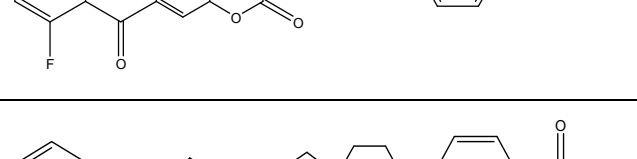
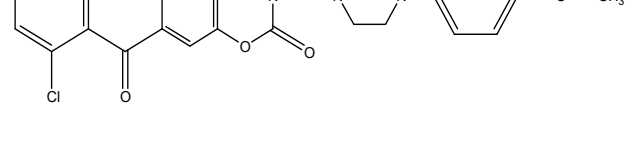
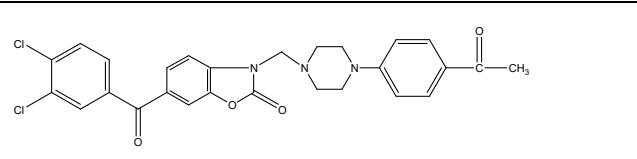
#### 3.2. Types of Benzoxazolinone Derivatives

The open formulas of the 3-(4-substituted piperazinomethyl) benzoxazolinone derivatives are given below (Table 3.1):

**Table 1.1. Structural formulas of the 3-(4-substituted piperazinomethyl) benzoxazolinone derivatives.**

#	Structural Formula	IUPAC Name
<b>HH01</b>		5-chloro-3-((4-(4-nitrophenyl)piperazin-1-yl)methyl)benzoxazol-2(3H)-one
<b>HH02</b>		6-benzoyl-3-((4-(4-nitrophenyl)piperazin-1-yl)methyl)benzoxazol-2(3H)-one
<b>HH03</b>		6-(2-fluorobenzoyl)-3-((4-(4-nitrophenyl)piperazin-1-yl)methyl)benzoxazol-2(3H)-one
<b>HH04</b>		6-(4-fluorobenzoyl)-3-((4-(4-nitrophenyl)piperazin-1-yl)methyl)benzoxazol-2(3H)-one

<b>HH05</b>		6-(3-chlorobenzoyl)-3-((4-(4-nitrophenyl)piperazin-1-yl)methyl)benzoxazol-2(3H)-one
<b>HH06</b>		3-((4-(benzo[d][1,3]dioxol-5-yl)piperazin-1-yl)methyl)-6-(2-fluorobenzoyl)benzoxazol-2(3H)-one
<b>HH07</b>		3-((4-(benzo[d][1,3]dioxol-5-yl)piperazin-1-yl)methyl)-6-(4-fluorobenzoyl)benzoxazol-2(3H)-one
<b>HH08</b>		3-((4-(benzo[d][1,3]dioxol-5-yl)piperazin-1-yl)methyl)-6-(3,4-dichlorobenzoyl)benzoxazol-2(3H)-one
<b>HH09</b>		6-(4-fluorobenzoyl)-3-((4-(pyridin-2-yl)piperazin-1-yl)methyl)benzoxazol-2(3H)-one
<b>HH10</b>		ethyl 4-((6-(4-fluorobenzoyl)-2-oxobenzoxazol-3(2H)-yl)methyl)piperazine-1-carboxylate
<b>HH11</b>		Ethyl 4-((5-chloro-2-oxobenzoxazol-3(2H)-yl)methyl)piperazine-1-carboxylate
<b>HH12</b>		ethyl 4-(4-((6-(3-fluorobenzoyl)-2-oxobenzoxazol-3(2H)-yl)methyl)piperazin-1-yl)benzoate

<b>HH13</b>		ethyl 4-(4-((2-oxobenzo[ <i>d</i> ]oxazol-3(2 <i>H</i> )-yl)methyl)piperazin-1-yl)benzoate
<b>HH14</b>		3-((4-(4-acetylphenyl)piperazin-1-yl)methyl)-5-chloro benzoxazol-2(3 <i>H</i> )-one
<b>HH15</b>		3-((4-(4-acetylphenyl)piperazin-1-yl)methyl)benzoxazol-2(3 <i>H</i> )-one
<b>HH16</b>		3-((4-(4-acetylphenyl)piperazin-1-yl)methyl)-6-(4-fluorobenzoyl)benzoxazol-2(3 <i>H</i> )-one
<b>HH17</b>		3-((4-(4-acetylphenyl)piperazin-1-yl)methyl)-6-(2-fluorobenzoyl)benzoxazol-2(3 <i>H</i> )-one
<b>HH18</b>		3-((4-(4-acetylphenyl)piperazin-1-yl)methyl)-6-(2-chlorobenzoyl)benzoxazol-2(3 <i>H</i> )-one
<b>HH19</b>		3-((4-(4-acetylphenyl)piperazin-1-yl)methyl)-6-(3,4-dichlorobenzoyl)benzoxazol-2(3 <i>H</i> )-one
<b>HH20</b>		5-chloro-3-((4-phenylpiperidin-1-yl)methyl)benzoxazol-2(3 <i>H</i> )-one

### 3.3. Chemicals Used in Analysis

Sodium hydroxide, sodium acetate, potassium chloride, acetonitrile phosphoric acid and disodium hydrogen phosphate were purchased from Sigma-Aldrich in Germany. Ammonium chloride, sodium dihydrogen phosphate, ammonium hydroxide, hydrochloric acid, acetic acid and methanol were supplied by Riedel de-Haen in Germany.

### 3.4. Equipments

Instruments/glasswares that have been used in this study as follows:

- ❖ Agilent Technologies 8453 UV-VIS Spectrophotometer
- ❖ Shimadzu 1280 UV-VIS Spectrophotometer
- ❖ Heidolph MR 3004 magnetic stirrer and heater
- ❖ OHAUS Analytical Plus Balances
- ❖ OHAUS Explorer 5 digits Balances
- ❖ Capp Autoclavable automatic pipettes (100-1000  $\mu\text{L}$ )
- ❖ Eppendorf automatic pipettes (100-1000  $\mu\text{L}$ )
- ❖ Agilent technologies rectangular quartz cell (10 mm and 3.5 mL)
- ❖ Oakton pH 2100 series pH-meter
- ❖ IsoLab , IsoTherm , MüllersLab volumetric flask (10, 25, 50, and 250 mL)
- ❖ Merck HC 748513 standard (pH:4, 7, 10)

### 3.5. Buffer solutions

Phosphoric acid-sodium dihydrogen phosphate buffer within pH 1.50-3.50 range was used by adjusting molarities and in suitable amounts and pHs. Acetic acid-sodium acetate buffer solution within pH 3.70-5.70 range was used. Molarities of acid and conjugated base were adjusted, and acetate buffer solutions in needed pHs were prepared. Phosphate buffer solution within pH 5.80-7.80 range was used. Disodium hydrogenphosphate and sodium dihydrogenphosphate ratios in suitable molarities were mixed. Ammonium chloride-ammonia buffer solution within pH 8.30-10.30 range was used. Ammonium chloride and ammonia ratios in suitable

molarities were mixed and needed acidities were prepared by adjusting concentrations of  $\text{NH}_4\text{Cl}$  and  $\text{NH}_3$ . The ionic strength was kept constant at 0.150 M.

### 3.6. Experimental methods

#### 3.6.1. Ultraviolet – Visible region (UV-VIS) spectroscopy method

In determination of acidity constants with UV-VIS spectrophotometric method, Shimadzu 1280 and Agilent 8453 UV-VIS Spectrophotometer devices were used. In spectrophotometric measurements, materials of benzoxazolinone derivatives (*HH01-HH20*) were prepared as  $1.00 \times 10^{-3}$  M in 10 mL capacity volumetric flasks, were weighed in a balance, and then dissolved in acetonitrile. Finally; the last concentration was completed to a 10 mL as  $0.75\text{--}3.00 \times 10^{-5}$  M with the buffer solution preferred (Buffer solutions were preserved in capped containers to prevent carbon dioxide absorbance and pure water was used). After waiting for the device to heat up, the buffer solution was added firstly into spectrophotometry's cell holder 10 mm quartz cuvette, and was left to measurement at room temperature (23 °C) as a blank sample. Then, samples of 3-(4-substituted piperazinomethyl) benzoxazolinone derivatives (*HH01-HH20*) were added into the quartz cuvette for measurement. Spectrum has been obtained. Then, absorbance-wavelength values obtained for each sample after the measurements were transferred to computer and put into charts. The best wavelength range was chosen among all pH values, and absorbance-pH charts of that wavelength were made.  $pK_a$  values of each compound were determined with these spectra obtained within 190-500 wavelength range in three independent experiments and three different wavelengths. The ionic strength was kept constant at 0.150 M at each pH value.

#### 3.6.2. Potentiometric method

In determination of acidity constants with potentiometric method, Mettler Toledo pH 2100 Series was used. The pH-meter was calibrated by a using standard pH 4.00 and pH 7.00 buffers. In titrimetric analysis, Isolab beaker and Heidolph MR Hei-Standard hot-plate and teflon stirrer were used. All solutions contain 8 mL water (was preserved in capped containers to prevent carbon dioxide absorbance), 3

M 0.5 mL potassium chloride and **HH01-HH20** resolved in 1.5 mL acetonitrile were prepared in a 25 mL beaker and were stirred at room temperature using a magnetic stirrer. The amount of acetonitrile was increased for some 3-(4-substituted piperazinomethyl) benzoxazolinone derivatives which have not dissolved well in this solution. Amount of acetonitrile were adjusted up to 20%. After that, pH of solution reduced less than 3 addition of HCl. As a result of the titrations performed with 0.01 M sodium hydroxide (NaOH), the pH values corresponding to the volumes used were recorded and put into charts, and then  $pK_a$  values were found. The ionic strength was kept constant at 0.150 M.



#### 4. RESULTS

To understand the chemical interaction between the compounds and their pharmacological effects, the acidity constant ( $K_a$ ) is a considerable important parameter. The link between  $K_a$  and the compound is used as a part of the investigations of new synthesis method for a drug candidate and in the explanation of the biopharmaceutics properties of these substances. Numerous biologically active organic compounds can be ionized mostly or entirely in physiologic medium. Biological activity and/or solubility are determined by the protonation center of the molecule.

For this reason,  $K_a$  values should be found with appropriate techniques for newly synthesized molecules. Hence, the main objective of this study is to find the acid dissociation constant values of twenty 3-(4-substituted piperazinomethyl) benzoxazolinone derivatives (**HH01-HH20**) using a spectrophotometric technique. Acidity constants acquired by this strategy are expected to be confirmed by other investigative technique, to be specific potentiometric titration.

To show the procedure applied in this study is correct, we have determined the  $pK_a$  value of 5-chlorobenzoxazolinone, which has been determined previously (Celik et al., 2013, p. 1589). In this study, the  $pK_a$  value of it was found to be  $8.23 \pm 0.04$  which is in good agreement with the published result in the literature (Celik et al., 2013, p. 1589).

After showing the procedure is correct, **HH01** that was structurally related to **HH02-05** was studied. These compounds pose p-nitro phenyl on the piperazine ring.  $pK_a$  value of **HH01** was determined to be 7.99 with UV-VIS spectrophotometry. In this study,  $pK_a$  values attained for **HH01-20** were given in Table 4.1 which has not been published in the literature.

Introducing phenyl group at the sixth position on the benzoxazolinone ring in the case of **HH02-05** compared to **HH01**, acidity constant values of them have been dropped from 7.99 to 7.41. This finding was observed for this group of compounds in the literature (Celik et al., 2013, p. 1589).

**Table 2.1. The experimental pK<sub>a</sub> values of 3-(4-substituted piperazinomethyl) benzoxazolinone derivatives.**

#	pK <sub>a</sub>		#	pK <sub>a</sub>	
	UV- Vis	Potentiometry		UV- Vis	Potentiometry
<b>HH01</b>	7.99±0.09	-	<b>HH11</b>	8.06±0.06	-
<b>HH02</b>	7.51±0.05	7.58±0.03	<b>HH12</b>	8.03±0.03	8.00±0.02
<b>HH03</b>	7.41±0.05	-	<b>HH13</b>	8.98±0.03	8.98±0.03
<b>HH04</b>	7.53±0.05	-	<b>HH14</b>	8.28±0.06	-
<b>HH05</b>	7.42±0.06	-	<b>HH15</b>	8.99±0.08	8.97±0.04
<b>HH06</b>	7.40±0.04	7.47±0.04	<b>HH16</b>	7.80±0.08	-
<b>HH07</b>	7.62±0.09	-	<b>HH17</b>	7.55±0.03	7.53±0.02
<b>HH08</b>	7.67±0.08	7.58±0.04	<b>HH18</b>	7.36±0.11	-
<b>HH09</b>	7.64±0.06	7.78±0.05	<b>HH19</b>	7.76±0.09	-
<b>HH10</b>	8.24±0.04	8.25±0.03	<b>HH20</b>	8.33±0.03	-

Absorption spectra obtained for **HH01** in different buffer at different pH values are given in Figure 4.1. Three absorption bands at 242 nm, 288 nm and 422 nm were observed. At these wavelengths, the absorbance values were observed to increase when the acidity of the solution decreased, and at pH above 10 remained constant.

The isosbestic points were seen in the spectrum means that **HH01** only gives one acid-base reaction (Figure 4.1). According to IUPAC definition, “isosbestic point

is usually employed with reference to a set of absorption spectra, plotted on the same chart for a set of solutions in which the sum of the concentrations of two principal absorbing components, A and B, is constant. The curves of absorbance against wavelength for such a set of mixtures often all intersect at one or more points, isosbestic points commonly appear when electronic spectra are determined on, either a solution in which a chemical reaction is in progress (in which case the two absorbing components concerned are reactant and product); or on a solution in which the two absorbing components are in equilibrium and their relative proportions are controlled by the concentration of some other component, typically the concentration of hydrogen ions, e.g., in acid base indicator equilibrium” (IUPAC, 1997).

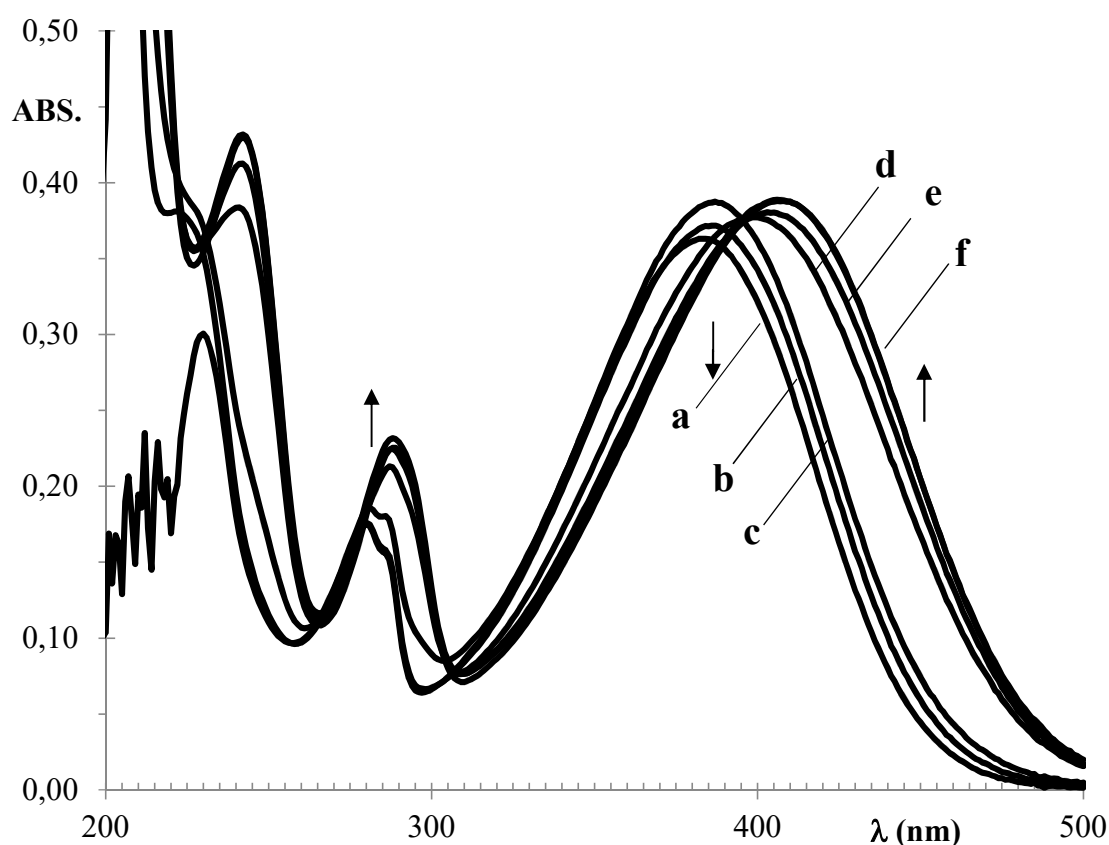


**Figure 3 Absorbance vs. wavelength plot for  $3 \times 10^{-5}$  M HH01 in various buffers. pH values: (a) 4.60, (b) 6.60, (c) 7.60, (d) 8.80, (e) 9.25, (f) 10.30.**

The plot of absorbance values as a function of pH for *HH01* is given in Figure 4.2 at the selected wavelength (288 nm). The obtained absorbance-pH plot is an S shaped type  $pK_a$  value of *HH01* at the mid-point of this curved line is 7.99. This value is the average of three replicate runs. The same and/or similar  $pK_a$  values were obtained at different wavelengths of the graphs.

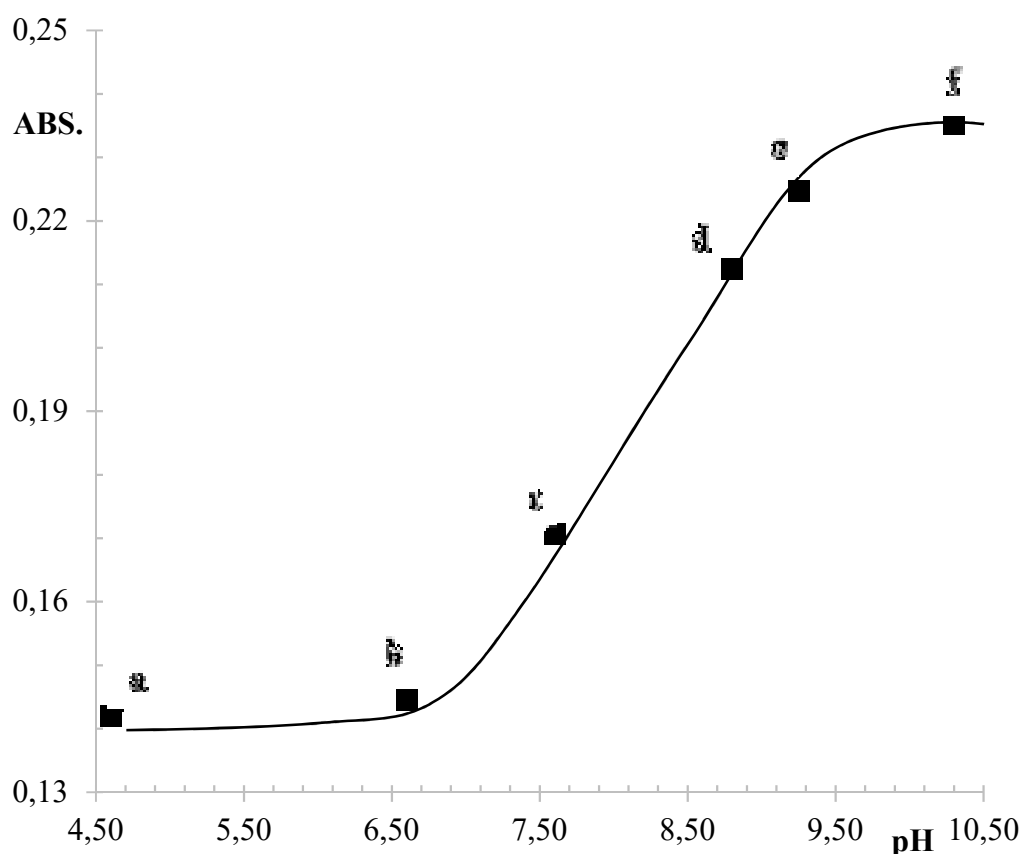


**Figure 4 Plot of absorbance as a function of pH for *HH01* at 288 nm. pH values: (a) 4.60, (b) 6.60, (c) 7.60, (d) 8.80, (e) 9.25, (f) 10.30.**

In order to check the accuracy of the  $pK_a$  values of *HH01* that has obtained by UV-VIS spectroscopy, the potentiometric titration was applied. In the potentiometric experiments, the ionic strength of the solution was fixed by using potassium chloride at 0.150 M. The concentration that was used in the potentiometric measurements had to be done higher than UV-VIS spectrophotometry to be able to see a change in the titration curve.

Due to the fact that the solubility of the *HH01* that have been worked on is decreased at higher concentration, only  $pK_a$  values of some 3-(2-Pyridylethyl) benzoxazolinone derivatives have been obtained by this method. The acidity constant values obtained by this method were gained by plotting pH vs. the volume of strong base added. An example of this plot is given in Figure 4.3 for *HH02*. The experimental data obtained by this method was repeated three times and the obtained average  $pK_a$  value is provided in Table 4.1.

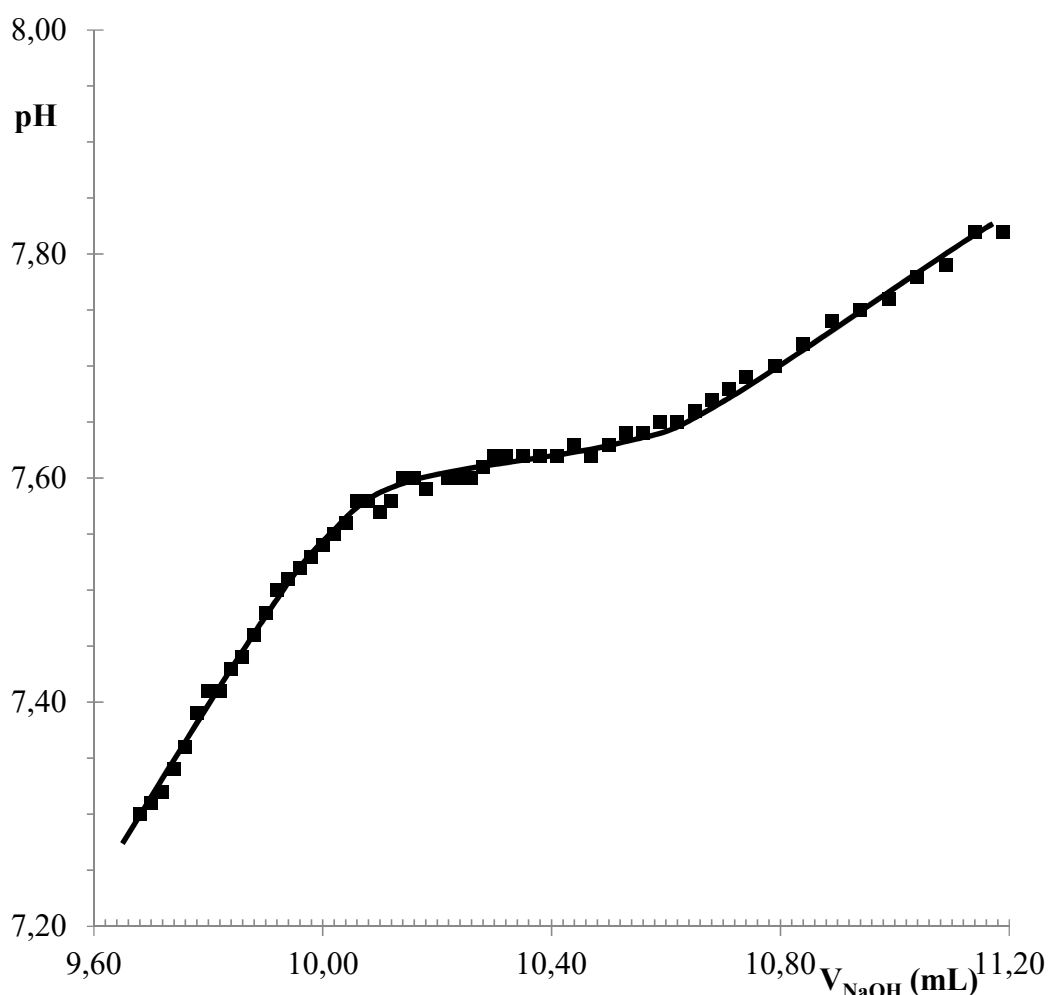


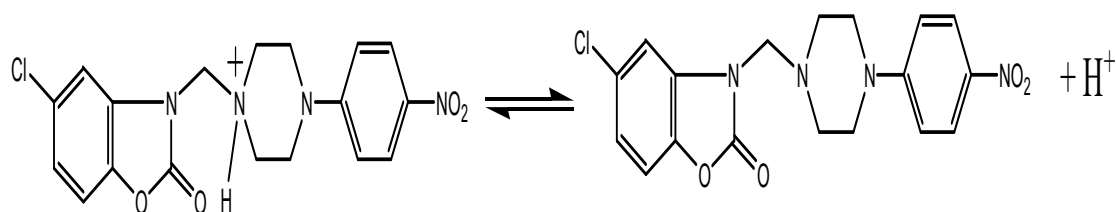
**Figure 5. Potentiometric titration curve for *HH02*.**

Acidity constant for *HH02* was found at the inflection point of the curved line in Figure 5.3 to be 7.58. There is surely the  $pK_a$  values obtained by the

potentiometric method and qualities acquired by UV-VIS spectroscopy are comparable. The experimental data obtained by this method was repeated three times and the obtained  $pK_a$  value are provided in Table 4.1.

It is found that the acid dissociation constant of value of *HH01* has relevance among the values provided in the literature (Celik et al., 2013, p. 1589) by means of two experimental approaches; and in order to understand the relationship between the structure of the compound and  $pK_a$ , this study have focused on the 3-(4-substituted piperazinomethyl) benzoxazolinone derivatives in a similar structure.

In view of the experimental confirmation, the equilibrium between protonated and unprotonated form can be given as follows (Scheme 1):



**Scheme 4.1. Equilibrium for the protonation of 3-(4-substituted piperazinomethyl) benzoxazolinone (*HH01*).**

In order to determine the acid dissociation constant values in the buffer solutions for *HH02-05*, two methods have been applied. The absorption spectra are given for *HH02* in Figure 4.4.

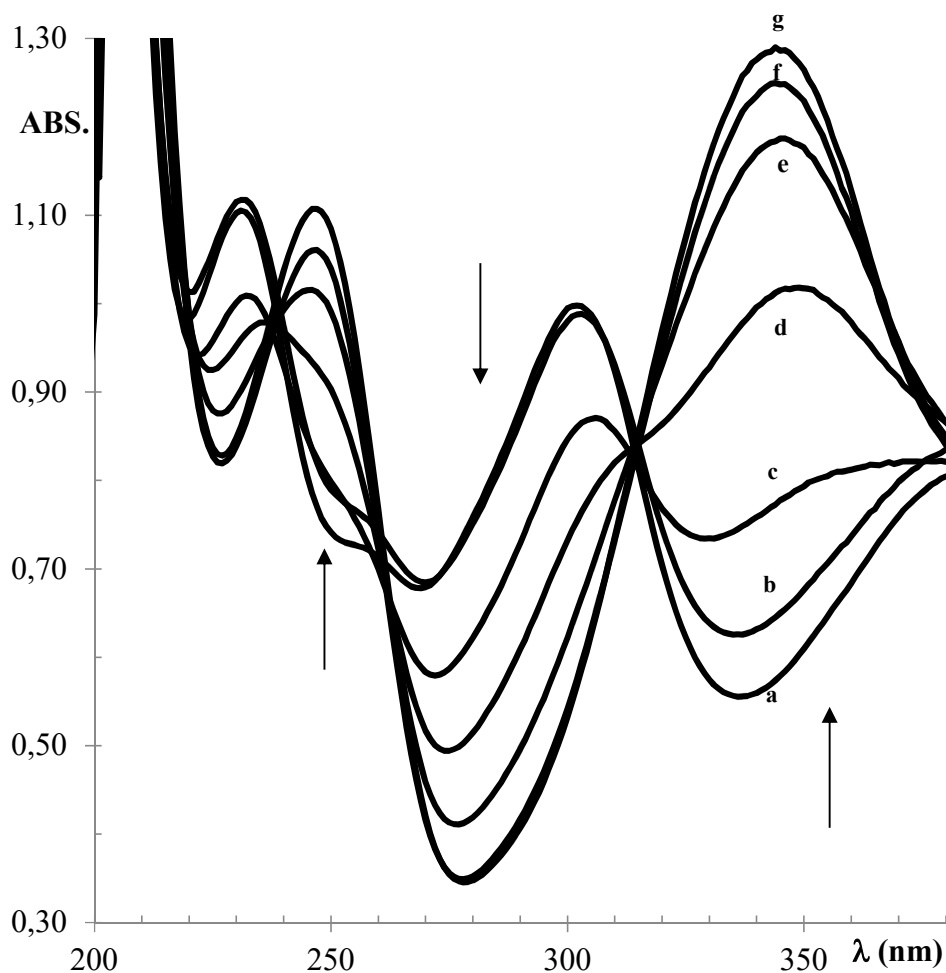


**Figure 6. Absorbance vs. wavelength plot for  $3 \times 10^{-5}$  M *HH02* in various buffers. pH values: (a) 6.15, (b) 6.60, (c) 7.20, (d) 7.70, (e) 8.30, (f) 8.80, (g) 9.25.**

When the absorbance values have increased by decreasing the acidity of the solutions at 330 nm, the compound has passed from the protonated form to neutral one. The absorbance-pH plot that was constructed at the 330 nm for *HH02* is given in Figure 4.5.

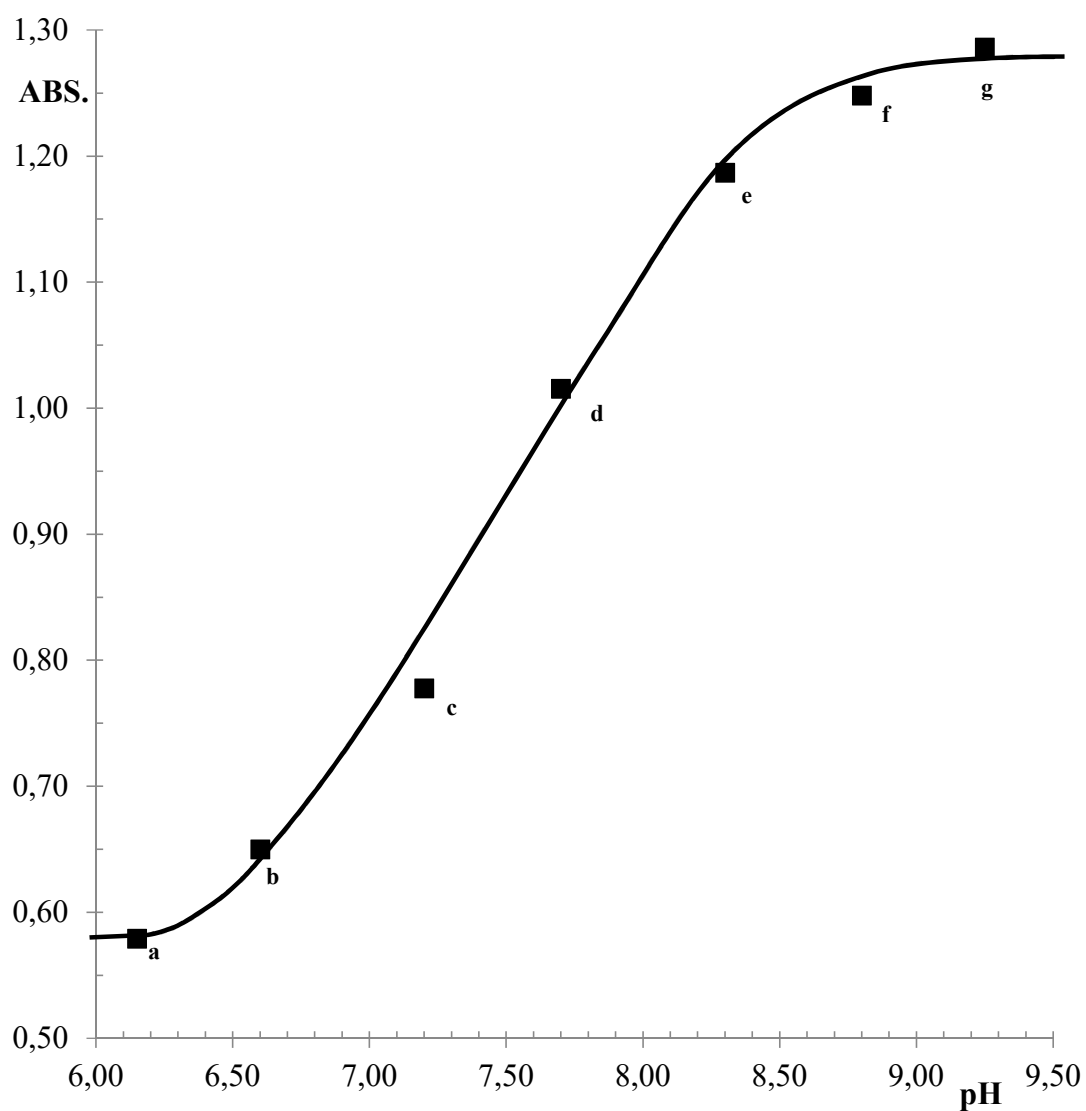


**Figure 7. Plot of absorbance as a function of pH for *HH02* at 330 nm. pH values: (a) 6.15, (b) 6.60, (c) 7.20, (d) 7.70, (e) 8.30, (f) 8.80, (g) 9.25.**

The curve obtained is in type of S-shaped and  $pK_a$  value of *HH02* from the mid-point of this curve has been determined as 7.51. As seen in Figure 4.5, the experimental data and theoretical curve has shown similarity on the harmony between the experimental results and theoretical values. The  $pK_a$  values were also calculated at 280 and 345 nm, and similar results were obtained. In order to check the



acidity constant, the same test has repeated at least three times and the average  $pK_a$  values were determined (Table 4.1).

After that, structurally related *HH06-08* have been studied. This group of compounds possess phenyl-1,2-dioxomethylene on the piperazine ring. Absorption spectra obtained for *HH07* is given as an example in Figure 4.6. The excellent isosbestic points, which have been previously described, were seen in spectra means that *HH07* only gives one acid-base reaction (Figure 4.6).

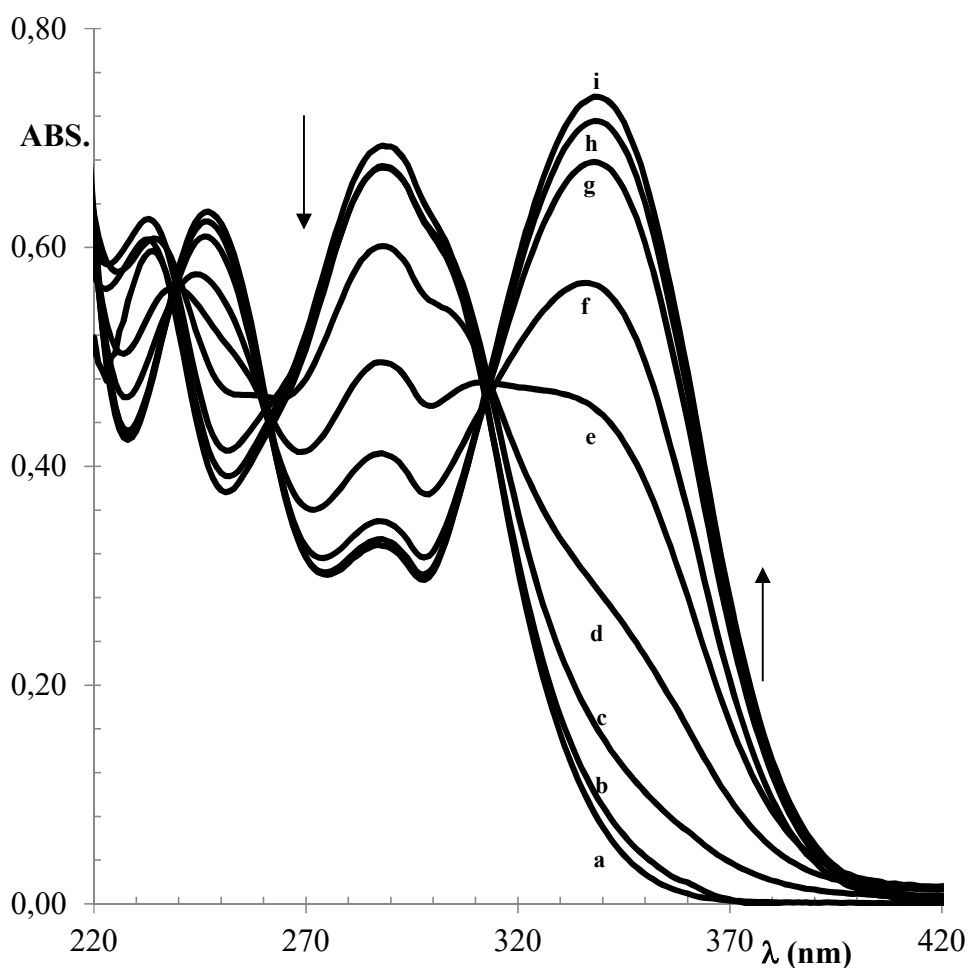


**Figure 8.** Absorbance vs. wavelength plot for  $3 \times 10^{-5}$  M *HH07* in various buffers. pH values: (a) 4.60, (b) 6.15, (c) 6.60, (d) 7.20, (e) 7.70, (f) 8.30, (g) 8.80, (h) 9.25, and (i) 9.70.

The absorbance-pH plot that was constructed at the 340 nm for **HH07** is given in Figure 4.7.

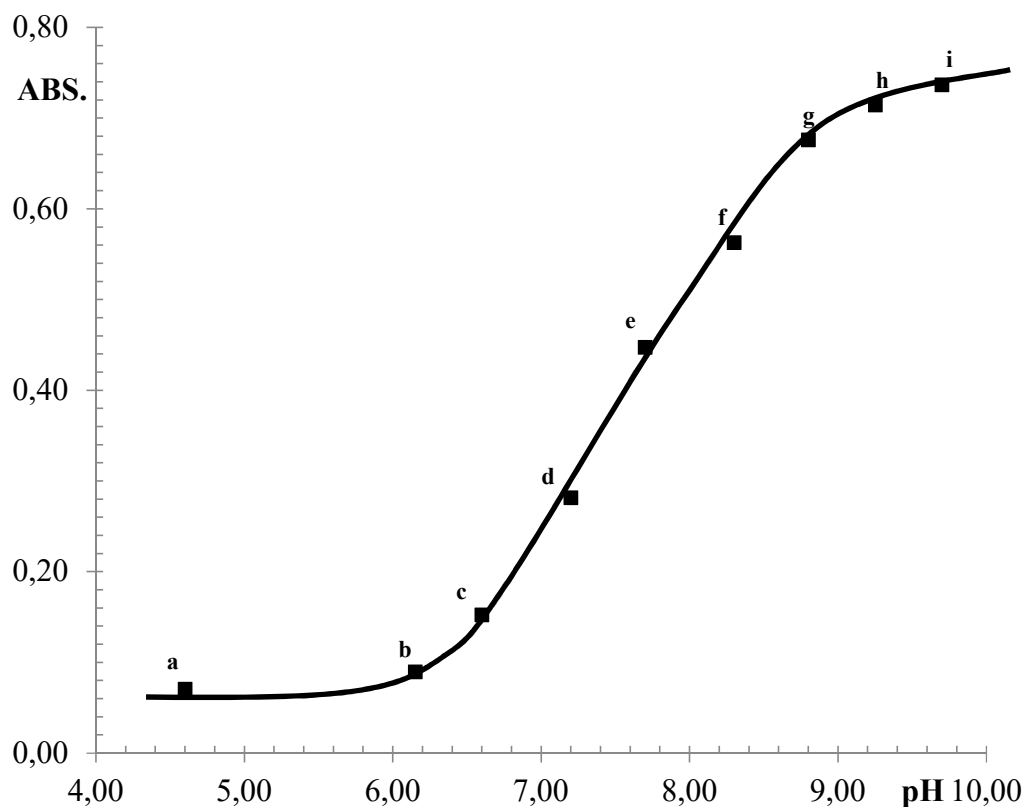


**Figure 9.** Plot of absorbance as a function of pH for **HH07** at 340 nm. pH values: (a) 4.60, (b) 6.15, (c) 6.60, (d) 7.20, (e) 7.70, (f) 8.30, (g) 8.80, (h) 9.25, and (i) 9.70.

The curve obtained is in type of S-shaped and  $pK_a$  value of **HH07** from the mid-point of this curve has been determined as 7.62. The  $pK_a$  values were also calculated at 285 and 350 nm, and similar results were obtained. In order to check the acidity constant, the same test has repeated at least three times and the average  $pK_a$  values were determined. The  $pK_a$  value is reported for **HH09** by using the same techniques in Table 4.1.

After finding the  $pK_a$  values of first nine compounds, the study was extended on the four structurally related compounds that contain an ethyl ester group on piperazine ring. Compounds **HH10-13** have been studied. Absorption spectra for

*HH13* are shown in Figure 4.8. The isosbestic points in the spectra mean that *HH13* gives only one acid-base equilibrium (Figure 4.8).

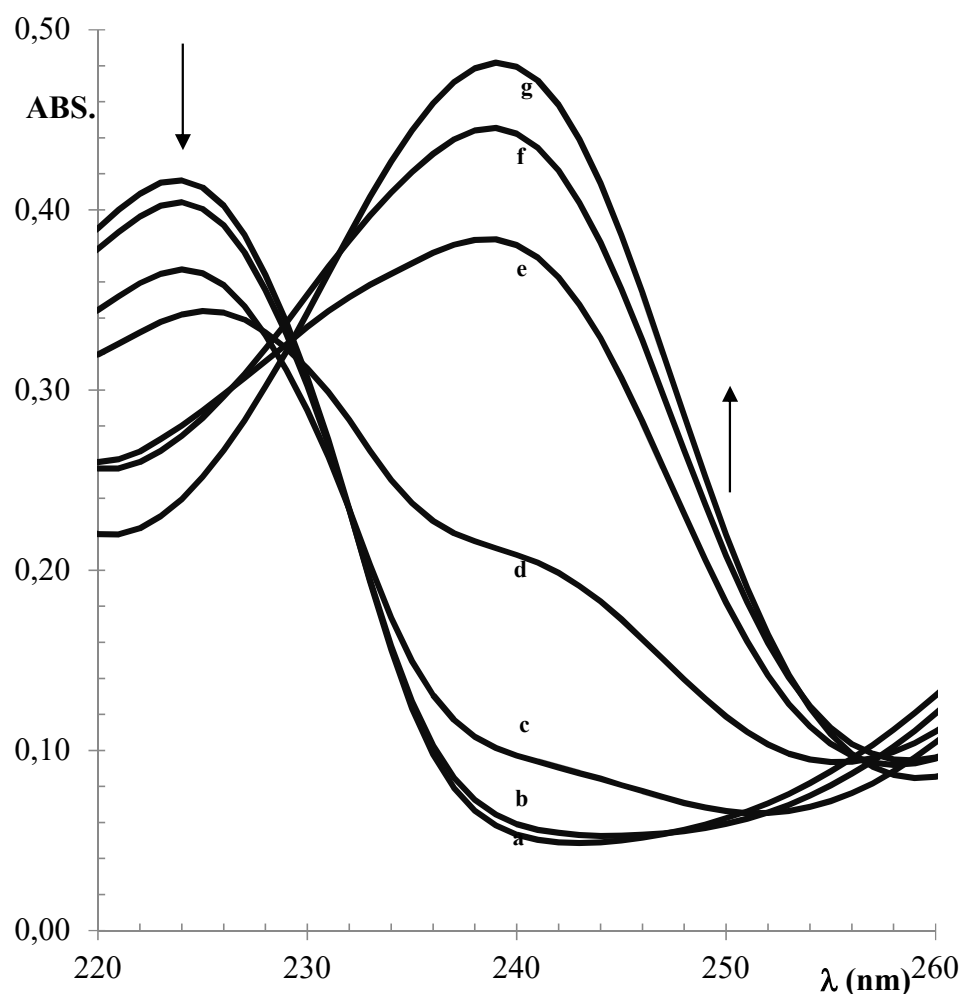


**Figure 10. Absorbance vs. wavelength plot for  $3 \times 10^{-5}$  M *HH13* in various buffers. pH values: (a) 6.25, (b) 7.35, (c) 8.30, (d) 8.80, (e) 9.45, (f) 9.80, and (g) 10.30.**

The potentiometric titration was applied for *HH13* due to the fact that it has been dissolved in the experimental condition. However, the concentration that is used in the potentiometric measurements has higher concentration than that of UV-VIS one. The solubility of the *HH13* decreased at higher concentration; thus, the amount of acetonitrile was increased to 20%. This experimental change helped us to

determine the  $pK_a$  value, which was extracted by plotting pH vs. the volume of NaOH. The obtained  $pK_a$  value is reported in Table 4.1. An example of this plot is given in Figure 4.9 for *HH13*.

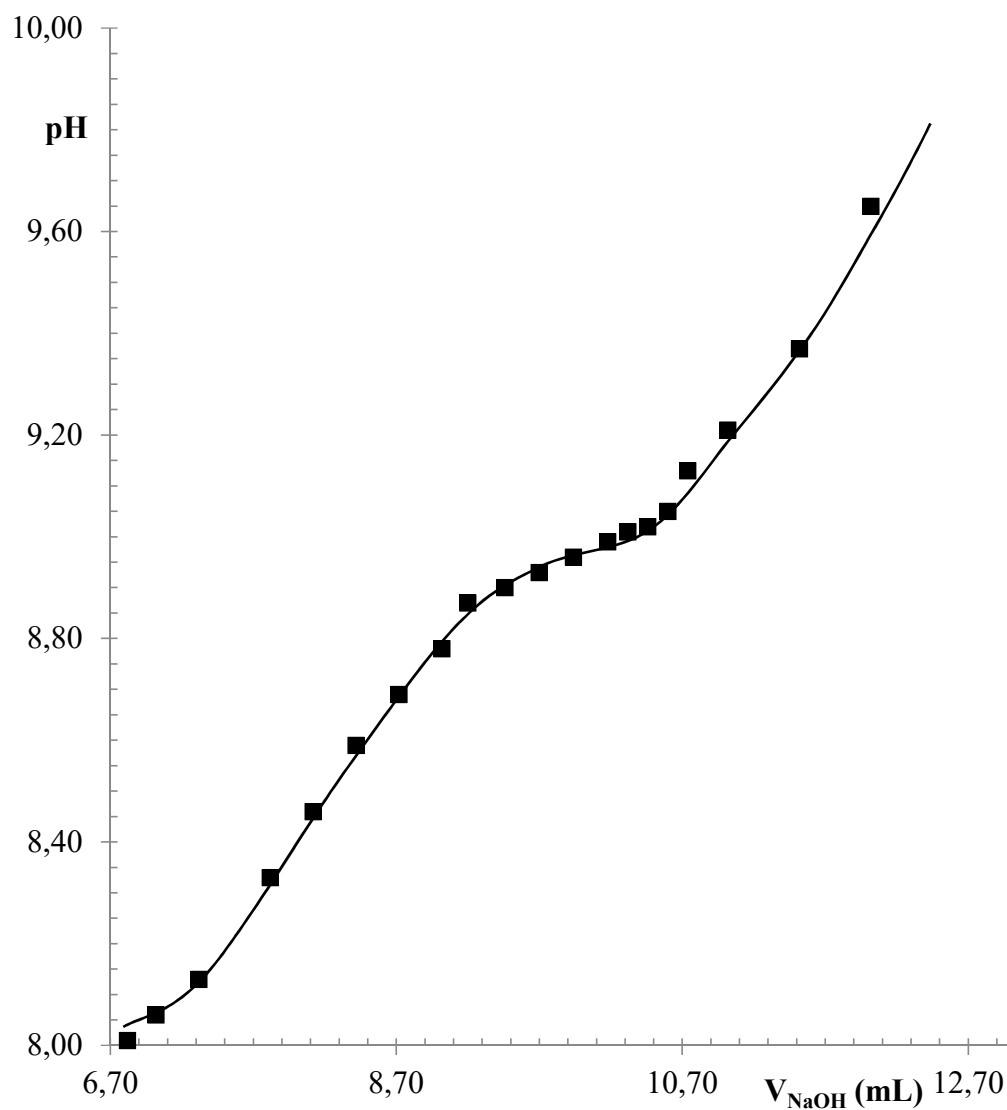


**Figure 11. Potentiometric titration curve for *HH13*.**

Next, we worked with six structurally related compounds that contain an acetyl group on the piperazine ring. Compounds *HH14-19* were studied to determine the acid dissociation constants. Absorption spectra are given in Figure 4.10 for *HH18* as an example.

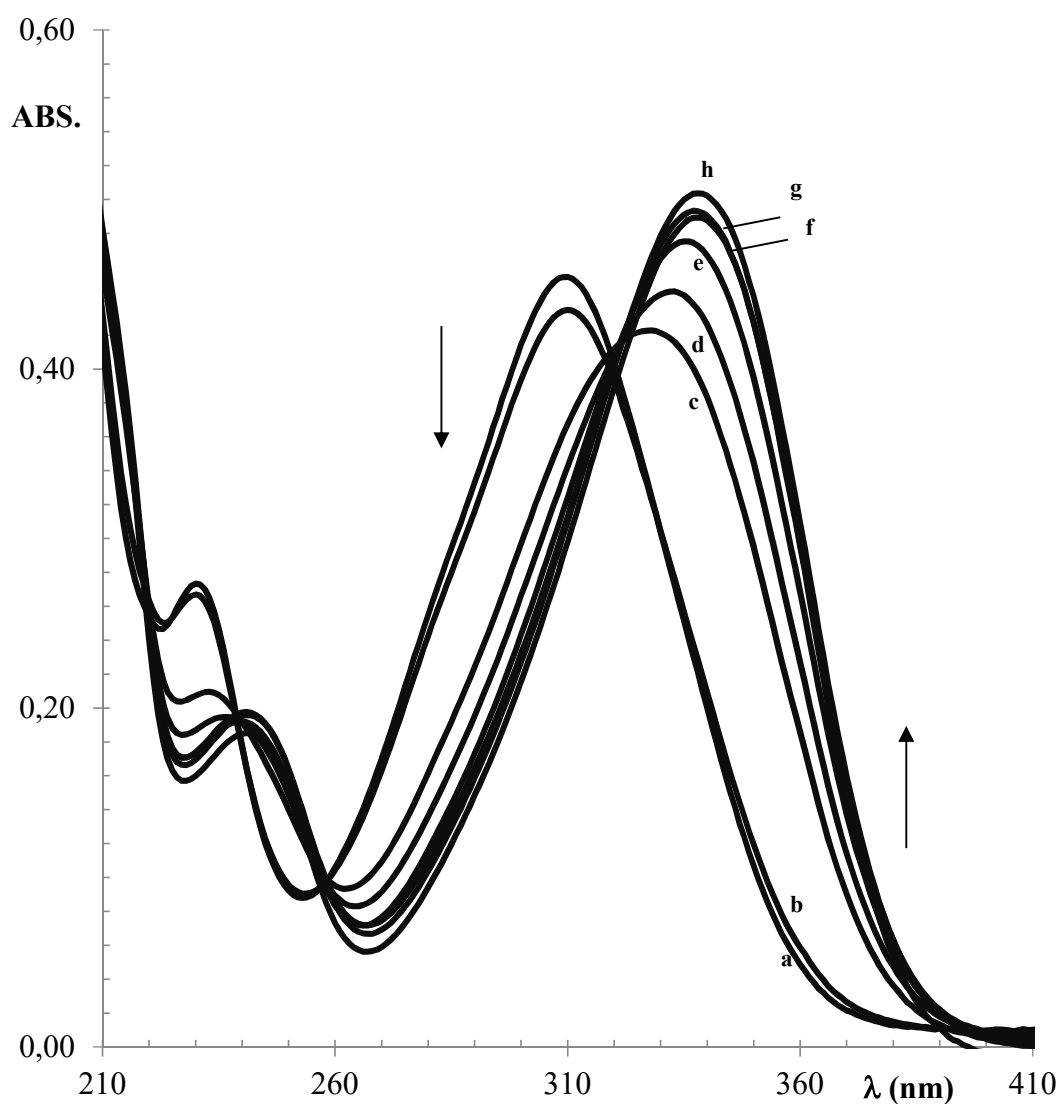


**Figure 12. Absorbance vs. wavelength plot for  $0.75 \times 10^{-5}$  M *HH18* in various buffers. pH values: (a) 5.75, (b) 6.25, (c) 7.80, (d) 8.30, (e) 8.80, (f) 9.45, (g) 9.80, and (h) 10.30.**

The last compound, *HH20*, was studied to determine not only its  $pK_a$  value but also get an idea about the position of the protonation. Potentiometry was turned out to be a meaningless method for this situation because of the low dissolution of *HH20* in an aqueous solution. The  $pK_a$  was founded by UV-VIS. Absorption spectra achieved for *HH20* are given in Figure 4.11.

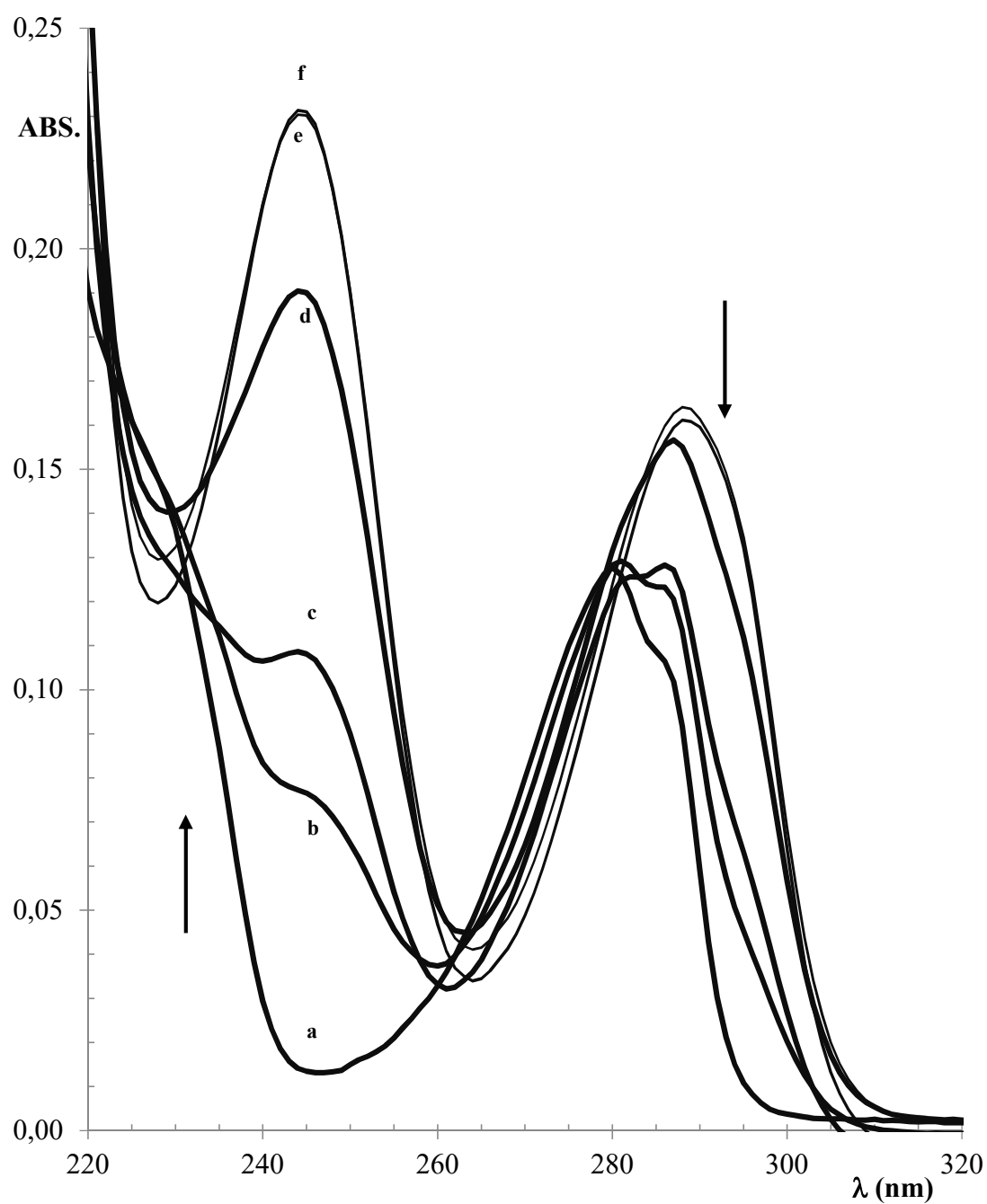


**Figure 13.** Absorbance vs. wavelength plot for  $1 \times 10^{-5}$  M *HH20* in various buffers. pH values: (a) 5.75, (b) 7.80, (c) 8.30, (d) 8.80, (e) 9.45, and (f) 9.80.

The absorbance-pH plot that was constructed at the 250 nm for *HH20* is given in Figure 4.12.

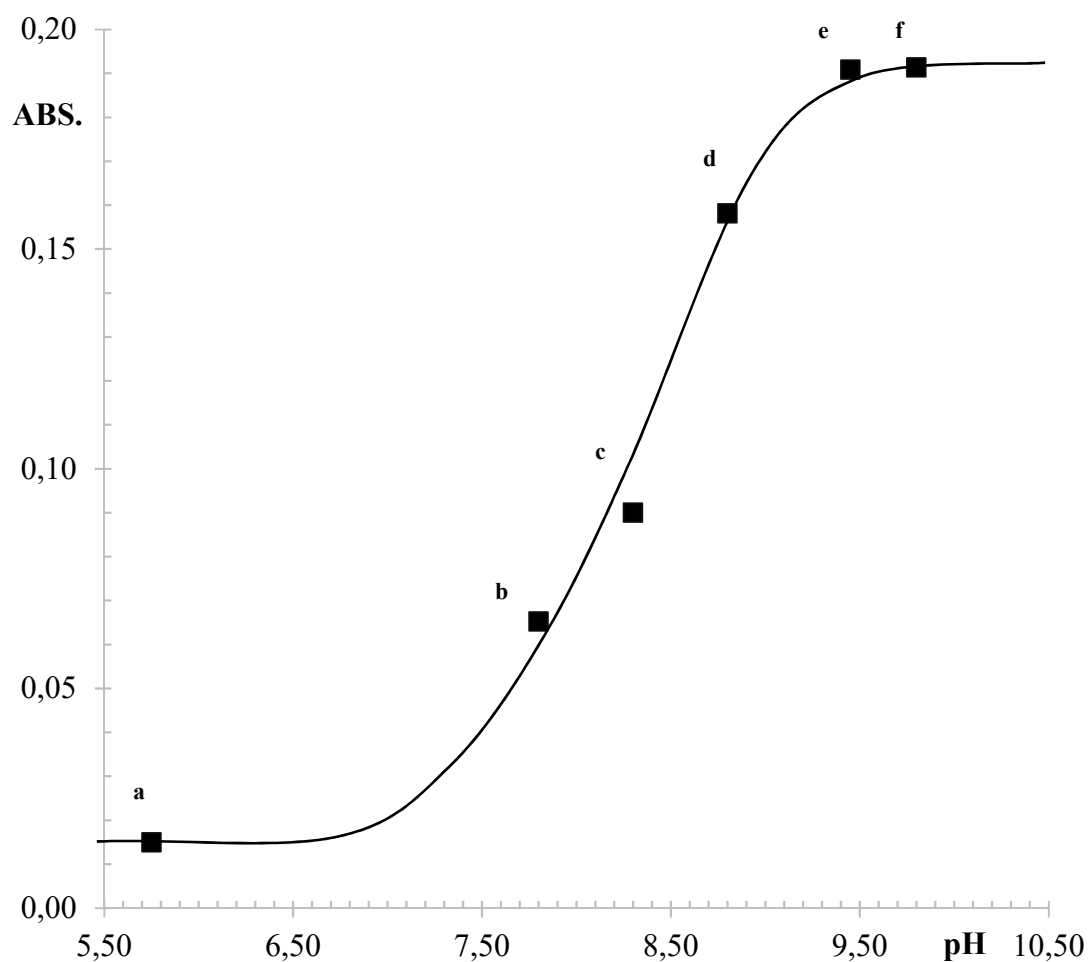


**Figure 14. Plot of absorbance values as a function of pH for *HH20* at 250 nm. pH values: (a) 5.75, (b) 7.80, (c) 8.30, (d) 8.80, (e) 9.45, and (f) 9.80.**

S-shaped absorbance-pH plot was also obtained. The acid dissociation constant for *HH20* was determined at the inflection point of this curved as 8.33. Similar results were obtained wavelengths at 244 and 295 nm. The average value is reported in Table 4.1.

## 5. DISCUSSION

The acid dissociation constants ( $pK_a$ ) values found from experiments with 3-(4-substituted piperazinomethyl) benzoxazolinone derivatives were reported in Table 4.1. UV-VIS spectrophotometry and potentiometric techniques have been used to determine the  $pK_a$  values of twenty structurally-related compounds (**HH01-20**).

It was suggested with the help of **HH20** that the protonation should be on the nitrogen atom of piperazine ring. This nitrogen atom is only place where the protonation can take place (Celik et al., 2013, p. 1589). Based on this, the studies regarding the main structure and derivatives in 5<sup>th</sup> and 6<sup>th</sup> positions have been carried out and it is assigned that 6-benzoyl derivatives are more acidic than main structure. The acid dissociation constant of **HH20** was found to be 8.33.

The structure-analgesic activity relationship of compounds was also examined in this study. The analgesic activity (Palaska et al., 1995, p. 693) was interrelated to the  $pK_a$  values of the studied molecules with comparison to acetylsalicylic acid (ASA). Analgesic activities of the studied compounds were reported in tables 5.1-6.1 (Palaska et al., 1995, p. 693). The analgesic activity of the compounds were screened by a "Modified Koster's Test" using ASA as a reference analgesic. As seen in table 5.1-6.1, the studied compounds showed analgesic activities higher than ASA except for **HH06** and **HH19**. We tried to correlate these finding with the acid dissociation constants.

When **HH01** is compared to **HH02-05**, **HH01** is more basic than 6-benzoyl derivatives (**HH02-05**) even though it contains a chlorine atom at the 5<sup>th</sup> position. It has been shown in the literature that benzoxazolinone with chlorine at the 5<sup>th</sup> is more acidic than that of no chlorine one (Celik et al., 2013, p. 1589). In terms of activity-acidity relationship, it is not suitable to compare **HH01-05** since **HH01** contains chlorine at the 5<sup>th</sup> position because the presence of chlorine atom at the 5<sup>th</sup> position has more activity than that of the unsubstituted one (Celik et al., 2013, p. 1589). Also, introducing a fluorine atom at the ortho position of benzoyl (**HH03**) is more



acidic than that of hydrogen derivative (*HH02*). Meantime, analgesic activity of *HH02* is lower than *HH03* (Table 5.1).

**Table 5.1. The p*K*<sub>a</sub> and analgesic activity values for *HH01*-*HH05* and ASA.**

#	p <i>K</i> <sub>a</sub>	% Analgesic Activity
<i>HH01</i>	7.99	65
<i>HH04</i>	7.53	53
<i>HH02</i>	7.51	46
<i>HH03</i>	7.41	62
<i>HH05</i>	7.42	64
ASA		47

The compounds, *HH06-08*, contain phenyl-1,2-dioxomethylene groups on the piperazine rings. It was observed that when their acidities decreased, their analgesic activities increased from 33 to 65 (Table 5.2). A small change of p*K*<sub>a</sub> of the compound almost doubles pharmacological activity. Also position of a fluorine atom on the benzoyl group has different acidity and also an analgesic activity as shown in Table 5.2.

**Table 5.2. The p*K*<sub>a</sub> and analgesic activity values for *HH06*-*HH08* and ASA.**

#	p <i>K</i> <sub>a</sub>	% Analgesic Activity
<i>HH06</i>	7.40	33
<i>HH07</i>	7.62	48
<i>HH08</i>	7.67	65
ASA		47

The compounds, *HH10-13*, contain ethyl ester groups on the piperazine rings. *HH13* is more basic than *HH11* (Table 5.3). The only difference between them is the presence of chlorine atom on the 5<sup>th</sup> position of benzoxazolinone ring of *HH11*. Introducing m-fluorabenzoyl group on the 6<sup>th</sup> position of benzoxazolinone ring (*HH12*) increases the acidity, but decreases the analgesic activity when compared to *HH13*.

**Table 5.3. The p*K*<sub>a</sub> and analgesic activity values for *HH10-HH13* and ASA.**

#	p <i>K</i> <sub>a</sub>	% Analgesic Activity
<i>HH13</i>	8.98	64
<i>HH10</i>	8.24	-
<i>HH11</i>	8.06	71
<i>HH12</i>	8.03	53
ASA		47

When comparing *HH10-13* with *HH02-05* bearing nitro group on the piperazine ring and with *HH06-09*, which possess phenyl-1,2-dioxomethylene group on piperazine ring, it can be seen that the availability of the ethyl ester group decreased the acidity of these compounds (Table 5.3).

*HH14-19* hold acetyl groups on piperazine rings. *HH14* is more acidic than *HH15* (Table 5.4). The only difference between them is the existence of a chlorine atom on the 5<sup>th</sup> position of benzoxazolinone ring of *HH14*. Introducing benzoyl group on the 6<sup>th</sup> position of benzoxazolinone rings decrease p*K*<sub>a</sub> values. Analgesic activities of these series compounds decreases as the acidities are increased (Table 5.4). Drastic drop in the analgesic activity can be seen for mono halogen containing benzoyl derivatives.

**Table 5.4. The p*K*<sub>a</sub> and analgesic activity values for *HH14-HH19* and ASA.**

#	p <i>K</i> <sub>a</sub>	% Analgesic Activity
<i>HH15</i>	8.99	81
<i>HH14</i>	8.28	96
<i>HH16</i>	7.80	65
<i>HH19</i>	7.76	41
<i>HH17</i>	7.55	54
<i>HH18</i>	7.36	50
ASA		47

## 6. CONCLUSION and RECOMMENDATION

The aim of this study was to find  $pK_a$  values of twenty 3-(4-substituted piperazinomethyl) benzoxazolinone derivatives by utilizing UV-VIS spectroscopy; and checking the accuracy of this method using potentiometry.

The position of the equilibrium reaction was suggested based on the experimental results. It is recommended with the assistance of *HH20* that the protonation ought to be on the nitrogen atom of the piperazine ring.

Under the light of data, the electron withdrawing atoms (fluorine or chlorine atom) on 6-benzoyl derivatives or on the main structure of benzoxazolinone ring showed more basic character. Acetyl substituted derivatives revealed more basic characters than the rest, and have given more pharmacological activities. When o-F-benzoyl derivatives (*HH03*, *HH06*, and *HH17*) were compared in terms of activity-structure relationship, *HH03* was found to be more active than *HH06*, and *HH17*. Even though  $pK_a$  values are similar, the presences of electron withdrawing atoms (fluorine) increase the acidity of the compound with respect to *HH02*. It was suggested that the *HH14* (acetyl substituted) has more basic character than that of *HH01* (nitro substituted) and *HH11* (ethyl ester substituted); meanwhile analgesic activities increase from *HH14* to *HH01* (see Table 6.1).

**Table 6.1. The  $pK_a$  and analgesic activity values for *HH01*, *HH11*, *HH14* and ASA.**

#	$pK_a$	% Analgesic Activity
<i>HH14</i>	8.28	96
<i>HH11</i>	8.06	71
<i>HH01</i>	7.99	65
ASA		47

Because of the acidic and / or basic character of the compounds that show different activities, the ionization degrees of them could be determined by pH values and acid dissociation constants. Based on this, relevant data could be extracted about availability of the groups, the biological activities, and prediction of solubility of studied organic molecules at a specified pH value. Experimental results of this study suggest that when the acid dissociation constant values of this group of compounds increase, analgesic activities of them increase. Compounds can be in the form of cationic, anionic or neutral form that influence the solubility, permeability, UV absorptions, and its reactivity. The ionized form is typically more water soluble, while the unprotonated form is less water-soluble and possesses higher membrane permeability.

The significant types of pharmaceuticals present in the medium can be assessed from the acidity constants. Thus, it is critical to know the dissociation constants for structurally related active pharmaceutical ingredients in order to determine their fate, occurrence and effects. Furthermore, the acid-base property of a drug candidate molecule is a key parameter for drug development progress because it controls absorption, distribution, metabolism, solubility as well as elimination.

The acidity constant is an important parameter. Because the passage of an organic molecule across the membranes and into cells is a function of physicochemical properties and that of the  $pK_a$  value. Therefore, one of the important step in the discovery of new drug candidate molecules requires an accurate experimental setup to obtain acid dissociation constant values. Some advanced analytical methods have been used for the determination of dissociation constants for active pharmaceutical ingredients. Besides from UV-VIS spectrophotometry and potentiometry; there are many other analytical methods such as liquid chromatography (LC), NMR titration, capillary zone electrophoresis (CZE), and capillary electrophoresis with mass detectors which are being used in the literature (Celik et al., 2013, p. 1589). Despite the fact that these strategies have brought a few

points of interest for finding the  $pK_a$  values, limitations such as expensive instrumental setup, sensitivity, and solubility of the compounds have been reported.

The UV–VIS spectrophotometric method could be used to determine  $pK_a$  values shown in this study as one of the best methods. The error of measurement of absorbance values at the specific wavelengths have to be reduced, and the studied buffer solutions must be selected at the most appropriate pH ranges to get consistent experimental results with this methodological approach. Likewise, the temperature of the surrounding area and the ionic strength should be retained constant during the course of the measurements. The volume of addition of base during the titration of the compounds with a base have to be selected cautiously and the acidity of the solution must be checked and recorded regularly even after the addition of small amounts for the potentiometric technique.

**REFERENCES:**

Albert, A., & Serjeant, E. P. (1984). Chelation and the stability constants of metal complexes. In the determination of ionization constants (pp. 176-191). Springer Netherlands.

Albert, A., & Serjeant, E. P. (1984). Determination of ionization constants by potentiometric titration using a glass electrode. In the determination of ionization constants (pp. 14-38). Springer Netherlands.

Allen, R. I., Box, K. J., Comer, J. E. A., Peake, C., & Tam, K. Y. (1998). Multiwavelength spectrophotometric determination of acid dissociation constants of ionizable drugs. *Journal of pharmaceutical and biomedical analysis*, 17(4), 699-712.

Allison, M. C., Howatson, A. G., Torrance, C. J., Lee, F. D., & Russell, R. I. (1992). Gastrointestinal damage associated with the use of nonsteroidal antiinflammatory drugs. *New England Journal of Medicine*, 327(11), 749-754.

Andrasi, M., Buglyo, P., Zekany, L., & Gaspar, A. (2007). A comparative study of capillary zone electrophoresis and pH-potentiometry for determination of dissociation constants. *Journal of pharmaceutical and biomedical analysis*, 44(5), 1040-1047.

Beltran, J. L., Sanli, N., Fonrodona, G., Barron, D., Özkan, G., & Barbosa, J. (2003). Spectrophotometric, potentiometric and chromatographic  $pK_a$  values of polyphenolic acids in water and acetonitrile–water media. *Analytica chimica acta*, 484(2), 253-264.

Bermann, M. C., Berthelot, P., Bonte, J. P., Debaert, M., Lesieur, D., Brunet, C., & Cazin, J. C. (1981). Chemical and pharmacological studies of anorectic drugs with phenylpiperazinyl structure. *Arzneimittel-Forschung*, 32(6), 604-610.

Bryant, A. E., Aldape, M. J., Bayer, C. R., Katahira, E. J., Bond, L., Nicora, C. D., & Stevens, D. L. (2017). Effects of delayed NSAID administration after experimental eccentric contraction injury—A cellular and proteomics study. *PloS one*, 12(2), e0172486.

Celik, H., Büyükağa, M., Çelebier, M., Turkoz Acar, E., Baymak, M. S., Gökhan-Kelekçi, N., & Erdoğan, H. (2013). Determination of  $pK_a$  values of some benzoxazoline derivatives and the structure–activity relationship. *Journal of Chemical & Engineering Data*, 58(6), 1589-1596.

Flowers, P., Theopold, K., & Langley, R. (2015). *Chemistry OpenStax College: Acid-base equilibria* (pp. 777-791). Houston, Texas, Rice University

Flowers, P., Theopold, K., & Langley, R. (2015). *Chemistry OpenStax College: Buffers* (pp. 821-838). Houston, Texas, Rice University

Dubois, R. N., Abramson, S. B., Crofford, L., Gupta, R. A., Simon, L. S., Van De Putte, L. B., & Lipsky, P. E. (1998). Cyclooxygenase in biology and disease. *The FASEB journal*, 12(12), 1063-1073.

Goldstein, J. L., Eisen, G. M., Lewis, B., Gralnek, I. M., Zlotnick, S., & Fort, J. G. (2005). Video capsule endoscopy to prospectively assess small bowel injury with celecoxib, naproxen plus omeprazole, and placebo. *Clinical Gastroenterology and Hepatology*, 3(2), 133-141.

Griffin, M. R., Yared, A., & Ray, W. A. (2000). Nonsteroidal anti-inflammatory drugs and acute renal failure in elderly persons. *American Journal of Epidemiology*, 151(5), 488-496.

Harvey, D. (2000). *Modern Analytical Chemistry* (Vol. 381). New York: McGraw-Hill.

Helmy, A. M. (1997). Electrochemical reduction of 3-phenyl azo-2, 4 (3H, 5H)-furanone at the DME. *Journal of Electroanalytical Chemistry*, 420(1-2), 259-266.

Henry, D., Page, J., Whyte, I., Nanra, R., & Hall, C. (1997). Consumption of non-steroidal anti-inflammatory drugs and the development of functional renal impairment in elderly subjects. Results of a case-control study. *British journal of clinical pharmacology*, 44(1), 85-90.

Hernández-Díaz, S., & Rodríguez, L. A. G. (2000). Association between nonsteroidal anti-inflammatory drugs and upper gastrointestinal tract bleeding/perforation: an overview of epidemiologic studies published in the 1990s. *Archives of internal medicine*, 160(14), 2093-2099.

Hernández-Díaz, S., Varas-Lorenzo, C., & García Rodríguez, L. A. (2006). Non-steroidal antiinflammatory drugs and the risk of acute myocardial infarction. *Basic & clinical pharmacology & toxicology*, 98(3), 266-274.

Jiménez-Lozano, E., Marqués, I., Barrón, D., Beltrán, J. L., & Barbosa, J. (2002). Determination of pK<sub>a</sub> values of quinolones from mobility and spectroscopic data obtained by capillary electrophoresis and a diode array detector. *Analytica Chimica Acta*, 464(1), 37-45.

Kearney, P. M., Baigent, C., Godwin, J., Halls, H., Emberson, J. R., & Patrono, C. (2006). Do selective cyclo-oxygenase-2 inhibitors and traditional non-steroidal anti-inflammatory drugs increase the risk of atherothrombosis? Meta-analysis of randomised trials. *BMJ*, 332(7553), 1302-1308.

Kean, W. F., & Buchanan, W. W. (2005). The use of NSAIDs in rheumatic disorders 2005: a global perspective. *Inflammopharmacology*, 13(4), 343-370.

Laine, L. (2001). Approaches to nonsteroidal anti-inflammatory drug use in the high-risk patient. *Gastroenterology*, 120(3), 594-606.

Langman, M. J. S., Weil, J., Wainwright, P., Lawson, D. H., Rawlins, M. D., Logan, R. F. A., & Colin-Jones, D. G. (1994). Risks of bleeding peptic ulcer associated with individual non-steroidal anti-inflammatory drugs. *The Lancet*, 343(8905), 1075-1078.

Lo, V., & Meadows, S. E. (2006). When should COX-2 selective NSAIDs be used for osteoarthritis and rheumatoid arthritis? *Clinical Inquiries, The Journal of Family Practice*, 55(3), 260-262.

Mamdani, M., Rochon, P., Juurlink, D. N., Anderson, G. M., Kopp, A., Naglie, G., & Laupacis, A. (2003). Effect of selective cyclooxygenase 2 inhibitors and naproxen on short-term risk of acute myocardial infarction in the elderly. *Archives of Internal Medicine*, 163(4), 481-486.

Ofman, J. J., MacLean, C. H., Straus, W. L., Morton, S. C., Berger, M. L., Roth, E. A., & Shekelle, P. (2002). A metaanalysis of severe upper gastrointestinal complications of nonsteroidal antiinflammatory drugs. *The Journal of Rheumatology*, 29(4), 804-812.

Palaska, E., Unlu, S., Ozkanli, F., Pilli, G., Erdoğan, H., Safak, C., & Duru, S. (1995). 3-substituted piperazinomethyl benzoxazolinones. Analgesic and anti-inflammatory compounds inhibiting prostaglandin E2. *Arzneimittel-Forschung*, 45(6), 693-696.

Pilli, G., Erdoğan, H., & Sunal, R. (1993). Some new benzoxazolinone derivatives with analgesic and anti-inflammatory activities. *Arzneimittel-Forschung*, 43(12), 1351-1354.

Pool, S.K., Patel, S., Dehring, K., Workman, H., & Pool, C.F., (2004). Determination of acid dissociation constants by capillary electrophoresis. *J. Chromatogr. A*, 1037, 445-454.

Qiang, Z., & Adams, C. (2004). Potentiometric determination of acid dissociation constants ( $pK_a$ ) for human and veterinary antibiotics. *Water research*, 38(12), 2874-2890.

Rodríguez, L. A. G., & Hernández-Díaz, S. (2003). Nonsteroidal anti-inflammatory drugs as a trigger of clinical heart failure. *Epidemiology*, 14(2), 240-246.

Skoog, D. A., Holler, F. J., & Nieman, T. A. (1998). *Principles of Instrumental Analysis*. Thomson Learning Inc., Toronto, ON, Canada.



Skoog, D. A., West, D. M., Holler, F. J., Crouch, S.R., (2013). *Fundamentals of Analytical Chemistry*. 9<sup>th</sup> ed., Brooks Cole, Belmont, USA.

Völgyi, G., Ruiz, R., Box, K., Comer, J., Bosch, E., & Takács-Novák, K. (2007). Potentiometric and spectrophotometric pK<sub>a</sub> determination of water-insoluble compounds: validation study in a new cosolvent system. *Analytica chimica acta*, 583(2), 418-428.

White, W. B., Faich, G., Borer, J. S., & Makuch, R. W. (2003). Cardiovascular thrombotic events in arthritis trials of the cyclooxygenase-2 inhibitor celecoxib. *The American Journal of Cardiology*, 92(4), 411-418.

Wolfe, M. M., Lichtenstein, D. R., & Singh, G. (1999). Gastrointestinal toxicity of nonsteroidal antiinflammatory drugs. *New England Journal of Medicine*, 340(24), 1888-1899.

Wróbel, R., & Chmurzyński, L. (2000). Potentiometric pK<sub>a</sub> determination of standard substances in binary solvent systems. *Analytica chimica acta*, 405(1), 303-308.

Zochling, J., van der Heijde, D., Dougados, M., & Braun, J. (2006). Current evidence for the management of ankylosing spondylitis: a systematic literature review for the ASAS/EULAR management recommendations in ankylosing spondylitis. *Annals of the Rheumatic Diseases*, 65(4), 423-432.

Zuniga, J. R., Phillips, C. L., Shugars, D., Lyon, J. A., Peroutka, S. J., Swarbrick, J., & Bon, C. (2004). Analgesic safety and efficacy of diclofenac sodium softgels on postoperative third molar extraction pain. *Journal of Oral and Maxillofacial Surgery*, 62(7), 806-815.

